U.S. DEPARTMENT OF COMMERCE / National Bureau of Standards

An Infrared Spectrometer Utilizing A Spin Flip Raman Laser, IR Frequency Synthesis Techniques, and CO_2 Laser Frequency Standards

NATIONAL BUREAU OF STANDARDS

The National Bureau of Standards [1] was established by an act of Congress March 3, 1901. The Bureau's overall goal is to strengthen and advance the Nation's science and technology and facilitate their effective application for public benefit. To this end, the Bureau conducts research and provides: (1) a basis for the Nation's physical measurement system, (2) scientific and technological services for industry and government, (3) a technical basis for equity in trade, and (4) technical services to promote public safety. The Bureau consists of the Institute for Basic Standards, the Institute for Materials Research, the Institute for Applied Technology, the Institute for Computer Sciences and Technology, and the Office for Information Programs.

THE INSTITUTE FOR BASIC STANDARDS provides the central basis within the United States of a complete and consistent system of physical measurement; coordinates that system with measurement systems of other nations; and furnishes essential services leading to accurate and uniform physical measurements throughout the Nation's scientific community, industry, and commerce. The Institute consists of the Office of Measurement Services, the Office of Radiation Measurement and the following Center and divisions:

Applied Mathematics — Electricity — Mechanics — Heat — Optical Physics — Center for Radiation Research: Nuclear Sciences; Applied Radiation — Laboratory Astrophysics [2] — Cryogenics [2] — Electromagnetics [2] — Time and Frequency [2].

THE INSTITUTE FOR MATERIALS RESEARCH conducts materials research leading to improved methods of measurement, standards, and data on the properties of well-characterized materials needed by industry, commerce, educational institutions, and Government; provides advisory and research services to other Government agencies; and develops, produces, and distributes standard reference materials. The Institute consists of the Office of Standard Reference Materials, the Office of Air and Water Measurement, and the following divisions:

Analytical Chemistry — Polymers — Metallurgy — Inorganic Materials — Reactor Radiation — Physical Chemistry.

THE INSTITUTE FOR APPLIED TECHNOLOGY provides technical services to promote the use of available technology and to facilitate technological innovation in industry and Government; cooperates with public and private organizations leading to the development of technological standards (including mandatory safety standards), codes and methods of test; and provides technical advice and services to Government agencies upon request. The Institute consists of the following divisions and Centers:

Standards Application and Analysis — Electronic Technology — Center for Consumer Product Technology: Product Systems Analysis; Product Engineering — Center for Building Technology: Structures, Materials, and Life Safety; Building Environment; Technical Evaluation and Application — Center for Fire Research: Fire Science; Fire Safety Engineering.

THE INSTITUTE FOR COMPUTER SCIENCES AND TECHNOLOGY conducts research and provides technical services designed to aid Government agencies in improving cost effectiveness in the conduct of their programs through the selection, acquisition, and effective utilization of automatic data processing equipment; and serves as the principal focus within the executive branch for the development of Federal standards for automatic data processing equipment, techniques, and computer languages. The Institute consists of the following divisions:

Computer Services — Systems and Software — Computer Systems Engineering — Information Technology.

THE OFFICE FOR INFORMATION PROGRAMS promotes optimum dissemination and accessibility of scientific information generated within NBS and other agencies of the Federal Government; promotes the development of the National Standard Reference Data System and a system of information analysis centers dealing with the broader aspects of the National Measurement System; provides appropriate services to ensure that the NBS staff has optimum accessibility to the scientific information of the world. The Office consists of the following organizational units:

Office of Standard Reference Data — Office of Information Activities — Office of Technical Publications — Library — Office of International Relations — Office of International Standards.

---

[1] Headquarters and Laboratories at Gaithersburg, Maryland, unless otherwise noted; mailing address Washington, D.C. 20234.

[2] Located at Boulder, Colorado 80302.

An Infrared Spectrometer Utilizing A Spin Flip Raman Laser, IR Frequency Synthesis Techniques, and CO$_2$ Laser Frequency Standards

t. Technical note, no. 670,

J.S. Wells and F.R. Petersen, Laser Metrology Section
Time and Frequency Division
National Bureau of Standards
Boulder, Colorado 80302

G.E. Streit , P.D. Goldan and C.M. Sadowski
Aeronomy Laboratory
National Oceanic and Atmospheric Administration
Boulder, Colorado 80302

CONTENTS

LIST OF FIGURES

An Infrared Spectrometer Utilizing a Spin Flip Raman Laser, IR Frequency Synthesis Techniques, and CO_2 Laser Frequency Standards

J. S. Wells, F. R. Petersen,
G. E. Streit, P. D. Goldan and C. M. Sadowski

The central part of this spectrometer is a cw spin flip Raman laser which operates between 1900 and 1800 cm^{-1}. The spin flip laser has so far demonstrated capabilities of resolving spectra separated by 0.01 cm^{-1} and shows promise of exceeding this resolution capability. When used with an opto-acoustic detector or with a detector and a flow system, it is capable of making a variety of measurements of environmental interest. Many of these environmental applications require only wavelength metrology.

By using CO_2 laser standards as frequency references and incorporating infrared frequency synthesis techniques, spectroscopy with the spin flip Raman laser can be put on a frequency metrology basis. A CO_2 laser has been used with a metal-oxide-metal diode to synthesize a known frequency reference which was used to stabilize the CO pump laser. The MOM diode also has the potential for measuring the frequency difference between the SFRL and the CO pump laser, a step which will complete absolute frequency measurements with the SFRL. The progress toward achieving this goal, the potential capabilities of this unique spectrometer, and some future applications are discussed.

Key words: Air quality measurements; improved resolution spectroscopy; infrared spectrometer; infrared frequency measurements; spin flip laser; tunable IR laser.

1. INTRODUCTION

As a result of continuing technological development in the laser field, tunable laser sources are now available and many new possibilities for high resolution infrared spectroscopy now exist. These tunable sources include the dye laser and parametric amplifiers in the visible, and diode lasers, spin flip Raman lasers (SFRL), and wave guide lasers in the infrared. The spectral brightness of these sources has precipitated a revolution in spectroscopy.[1]

We have constructed a cw spin flip laser which operates between 1900 and 1800 cm^{-1}. This spin flip laser has, so far, demonstrated capabilities of resolving spectra[2] separated by 0.01 cm^{-1} and shows promise of exceeding this

resolution. When spin flip laser technology is combined with the infrared frequency synthesis technology developed at NBS,[3] one has the potential for a unique infrared spectrometer. This spectrometer is being developed in the following manner. Because of the absolute frequency measurement[4] and stabilization work[5] with CO_2 lasers, excellent secondary standards in the intermediate IR spectral region now exist. One CO_2 device has been used with a metal-oxide-metal diode to synthesize a frequency reference with which to stabilize the CO pump for the spin flip Raman laser and thus provide the requisite accuracy and long term stability required for high resolution spectroscopy and chemical kinetic studies. The diode has also demonstrated a potential for measuring the frequency difference between the spin flip laser and its pump, a step which will permit absolute frequency measurements. High resolution spectroscopy and absolute frequency measurements are extremely useful for characterizing potential lasers and molecular species of high scientific and technological interest.

Our group also has a novel NOAA developed opto-acoustic (OA) detector which is capable of measuring infrared absorption in gases at relative concentrations well below a part per million.[6] This detector is very useful for doing spectroscopy on atmospheric pollutants and could be advantageous for investigations of compounds of low volatility in technological applications.

The capabilities with laser stabilization, infrared frequency synthesis, and high resolution spectroscopy, along with the spin-flip laser and the new detector provide us with unique opportunities to do some rather diverse experiments. The spin flip laser, stabilized lasers and opto-acoustic cell are combined into the spectroscopic system shown in Figure 1.

$$2 \times \nu_{CO_2} - \nu_{CO} = \nu_{\mu}\text{WAVE}$$

Figure 1. Block diagram of tunable laser spectrometer currently under development. The scheme for stabilizing the spin flip Raman laser (SFRL) pump is shown at the upper left. Shown at the right of the InSb resonator are two different detection schemes which have been used in the system. The stylized arrangement below the center indicates a back reflected pump signal and SFRL output going to a metal-on-metal diode. The goal of routinely beating these two signals together for a frequency difference measurement still requires some additional development.

3

Some potential applications using this system are:

Category I   (Environmental Problems)

1. Point sampling of atmospheric pollutants.
   (laboratory spectra on collected samples)

2. Evaluation of the OA detectors for field use.

3. Measurement of chemical kinetic rates.

Category II   (Metrology Problems)

1. Establishment of bench mark frequencies for laser diode users.
   (moderate resolution)

2. Measurement frequencies in molecules involved in saturated
   absorption experiments (high resolution)

3. Measurement of frequencies in molecules with potential for non-
   linear lasers (e.g. molecules where the energy level of interest
   is the sum of two CO_2 laser frequencies, i.e. NH_3, SiF_4, CH_3F, etc.)

4. Updating conventional molecular spectroscopy on molecules of high
   scientific interest.

These applications will be discussed in some detail after the following descrip-
tion of the spectrometer and its associated technology.

4

2. SPIN FLIP RAMAN LASER CHARACTERISTICS

Since many excellent references exist on the spin flip laser,[7,8,9] only a rudimentary sketch of the theory will be given. Our objective is to indicate how the experimental variables at one's disposal (magnetic field, pump frequency, input power, carrier concentration, temperature control technique, and InSb resonator size) are related to the performance of the spin flip Raman laser (SFRL). We also point out some limitations of the laser[10,11] that are generally not widely publicized, as well as advantages for certain applications.

A useful model in describing the Raman scattering[12] is indicated in Fig. 2. The magnetic field splits the Landau levels into electron spin down and spin up levels as shown. One of the requirements for spin flip lasing is that the magnetic field be strong enough to lift the upper spin level (spin down) above the Fermi level. The magnetic field at which this occurs is called the quantum limit. The diagram on the left indicates a field below the quantum limit.

With the upper level above the Fermi level as shown on right hand side, one can view the Raman scattering process as one in which the pump photon of energy $h\nu_p$ is absorbed, exciting an electron from the valence band to the empty upper level, leaving a hole in the valence band. This hole is filled by an electron from the lower Landau level (spin up) which drops down to fill the hole along with the emission of a photon of energy $h\nu_s$ which is shifted from the pump photon by $g^*\beta H$. This whole process (non-zero matrix elements of the dipole operator between the conduction band, with its pure spin up or spin down states, and the valence band) is made possible by the fact that the valence band state is a linear combination of spin up and spin down states. This mixed spin state is due to the spin-orbit interaction. At the end of the process

5

ENERGY vs ELECTRON MOMENTUM IN InSb

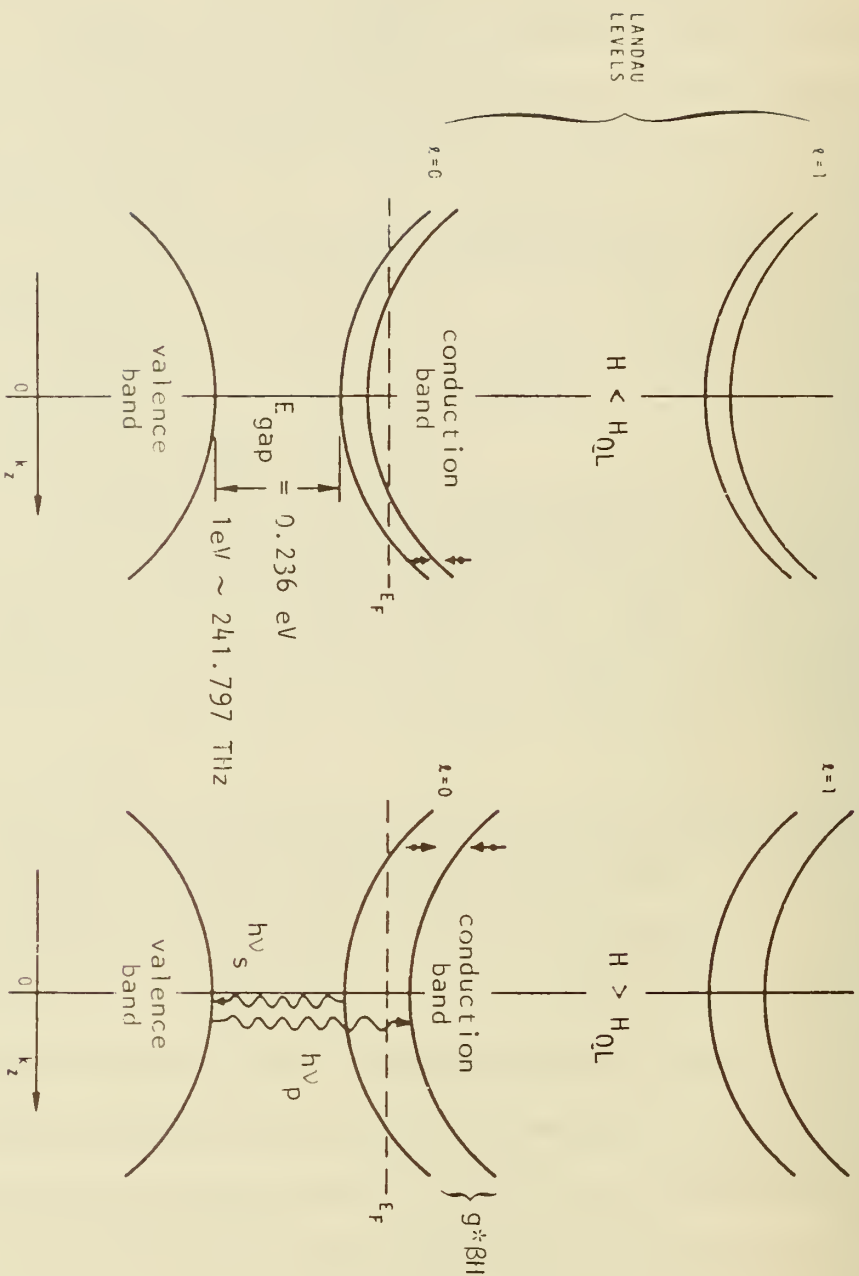Figure 2. Simplified diagrams of energy level versus electron momentum for indium antimonide. The splitting of the valence band into P3/2 and P1/2 levels is not shown. The energy gap between the valence band the conduction band shown is 0.236 electron volts, which corresponds to 5.20 μm, 1900 cm^{-1} or 56.8 THz. The Fermi level E_F indicated by the dashed line is a function of electron concentration in the material.

there is one more electron in the upper level and one less in the lower level; hence the net effect of the process is to flip the spin of one electron in the conduction band. The more general process involves virtual transitions and the exact match between photons and energy levels suggested in Fig. 2 is not required.

The spontaneous output frequency, ν_s, is given by

$$\nu_s = \nu_p \pm g^* \beta H$$

where ν_p is the pump frequency, g^* the effective g-factor, β is the Bohr magneton, and H the magnetic field intensity. Using an effective g-factor of 45, one gets an approximate value of 23 cm^{-1} per Tesla for a tuning rate.

In practice, the fact that the InSb is a resonator complicates the tuning rate. Modes in the resonator have frequencies, ν_R, given by

$$\nu_R = \frac{c}{2Ln} m$$

where c is the speed of light, L is the resonator length, n is the index of refraction, and m is an axial mode number. For a 7mm long InSb cavity, this mode spacing is about 5.35 GHz or 0.0075 Tesla.

Because of the existence of these cavity modes the output frequency of the spin flip laser is not the same continuous function of magnetic field as is the spontaneous frequency indicated by ν_s. As the magnetic field is swept, the output frequency may change at a rate less than predicted for ν_s, then hop in a discontinuous manner to the next higher frequency mode. These features are referred to as mode pulling and mode hopping.[13] They result from competing processes due to the discrete modes in the indium antimonide resonator.

7

The output frequency is given by the expression[13]

$$\nu = \frac{\nu_R \Gamma_s + \nu_s \Gamma_R}{\Gamma_s + \Gamma_R}$$

where Γ_R is the resonator linewidth and Γ_s is the spontaneous linewidth for the Raman scattering process. (Γ_s is approximately the lasing bandwidth for the spin flip laser). Typical values are 0.15 cm^{-1} for Γ_R and 0.04 cm^{-1} for Γ_s for electron concentrations on the order of 8×10^{15} cm^{-3}.

In practice, one can operate in the so called spin-saturation regime[14] (where the power is limited by the relaxation rate from the spin down to spin up level) with several closely spaced off-axis modes operating simultaneously and this mode hopping behavior is not discernible. The resulting linewidth (the order of 0.01 cm^{-1}) is still often less than pressure broadened lines of gases of interest in certain applications, as is shown later.

The coarse tuning is accomplished by pumping the spin flip laser with different CO laser transitions. This method turns out to be preferable in some instances to large tuning with a super conducting magnet for reasons appearing in the next paragraph. The preceeding discussion indicates the obvious frequency dependence on the pump frequency and magnetic field. A more subtle magnetic field dependence relating to the intensity appears in the following discussion.

In order to operate at frequencies far from the energy gap, i.e., about 50 to 200 cm^{-1} away, it is necessary to consider the lasing condition,[14]

$$R \exp\left[(G-\alpha) \ L\right] \geq 1$$

where G and α are the gain and loss per unit length, L is the resonator length and R is the sample reflectance. Of particular importance in this expression is the gain:

$$G = \left[\frac{4c^2}{h\nu_p^3 n^2}\right] N_e \frac{SI_o}{\Gamma_s} \ ,$$

where I_o is the intensity at the crystal which depends on the pump power available and the f number of the input lens. The resonance enhancement factor, S, is given by:

$$S = A \left[\frac{1}{\frac{\nu_r}{\nu_p} - \frac{\nu_p}{\nu_r}}\right]^2$$

where $h\nu_r \ (H) = E_g + (\ell + \frac{1}{2}) \ h \ \omega_c^* \ (H) + \frac{1}{2} \ g^*\beta H$. Those quantities not previously defined include, ℓ, the orbital quantum number, A, a constant of the order of 2.3×10^{-23}, and N_e the excess (spin up over spin down) electron concentration. The product $h \ \nu_r(H)$ is the energy difference between the top of the valence band and the bottom of the upper spin state of the particular Landau level (and hence depends on magnetic field) involved in the scattering process. The dependence of ν_r on H may (depending on sample concentration) dictate keeping H small and accomplishing the gross tuning by selecting a pump frequency ν_p closer to the desired SF frequency.

The resonance factor presents some difficulties as one moves away from the energy gap. Table 3 indicates the relative value of S/ν_p^3 at different pump frequencies. The most effective method of compensating for the

TABLE I

ν_P^3	ν_r/ν_P	ν_P/ν_r	S	$\dfrac{S}{S_o} \times \dfrac{\nu_{Po}^3}{\nu_P^3}$
1893	1.01	0.990	2500	1
1860	1.028	0.973	330	.139
1830	1.045	0.957	129	.058
1800	1.062	0.942	69	.031
1770	1.080	0.926	42	.021
1740	1.099	0.910	28	.014
1710	1.118	0.894	20	.011

With a 0.5 Tesla field, ν_r is about 1912 cm^{-1}. We aribtarily choose S_o to be defined at the widely used pump frequency of 1893 cm^{-1}. The above table shows the ratio of $\dfrac{S\nu_{Po}^3}{S_o\,\nu_P^3}$ for several pump frequencies between 1900 and 1700 cm^{-1}.

decreased gain at lower frequencies is to increase the pump intensity, however some limitations exist here. One can also increase the carrier concentration, however this is partially compensated by an increase in the spontaneous linewidth Γ_s. Γ_s and the Fermi level are related to the carrier concentration by the following proportionality.[15]

$$\Gamma_s \; \alpha \; E_F \; \alpha \; (N_e)^{2/3}$$

Since the Fermi level is also related to the carrier concentration, the upper spin level moves through the Fermi level at different magnetic fields for different concentrations. The Fermi level also is somewhat magnetic field (as well as temperature) dependent. The primary practical results relate to two considerations. One is the power output as a function of magnetic field. This is best illustrated by Fig. 3 which shows some results by the Heriot Watt group.[16] The spin flip laser power output is plotted vs magnetic field for two different electron concentrations. For some experiments, it is desireable to have the most power possible at 0.2 Tesla,[2] hence a 2.5 x 10^{15}/cm^3 sample is preferable. A second consideration is to obtain the narrowest possible linewidth. In this case it is advantageous to choose a low concentration sample where Γ_s and the gain bandwidth are smaller. In this case, it would also be preferable to select the spectral feature of interest to be close to the InSb band gap.

Several different techniques exist for cooling the InSb resonator to the desired 2K to 20K region. One technique is to use a commercial cryogenic refrigerator if one's budget permits this initial investiment. The other two methods involve the use of liquid helium, either for immersion in the
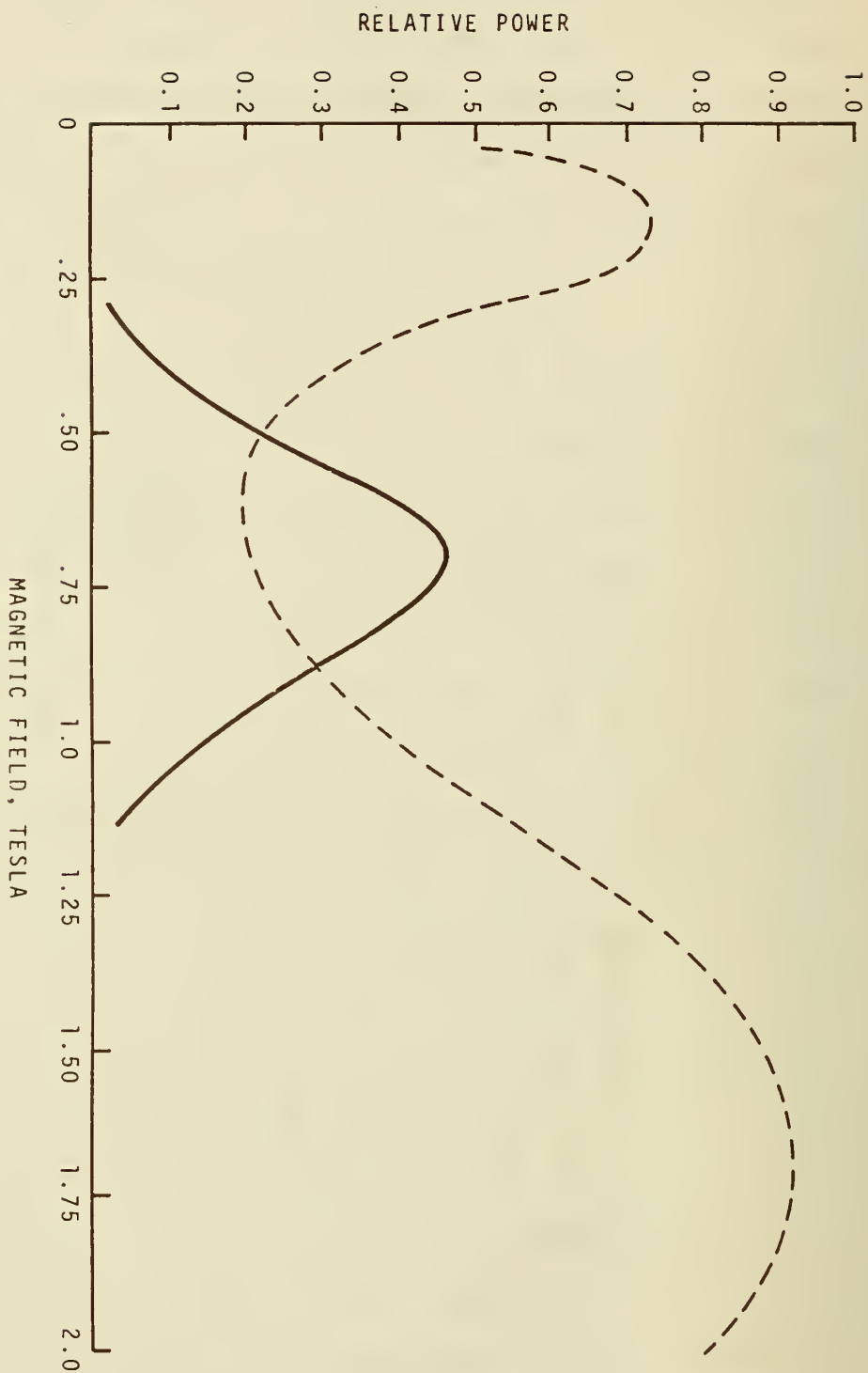
11

Figure 3. Relative power output vs magnetic field for two different concentration samples. The solid curve corresponds to an 8.5×10^{14} cm^{-3} sample and the single peak corresponds to the $\chi = 0$ Landau level sweeping thru the Fermi level. The dashed curve corresponds to 4.6×10^{15} cm^{-3} sample and in addition to the $\chi = 0$ peak at 1.7 Tesla, a peak also exists at 0.2 Tesla corresponding to the $\chi = 1$ Landau level sweeping past the Fermi level. One obviously has more power available from the higher concentration sample at select fields. The highest power output still occurs at fields attainable with a conventional magnet. The pump frequency here was around 1888 cm^{-1}. (Reproduced by permission)

liquid, or cooling by a cold finger. Each technique has both advantages and drawbacks. We have used both techniques in our operation.

For immersion, we have found ZnS windows sealed with a suitable low temperature epoxy to give fairly reliable operation, although a vacuum failure may occur upon repeated recycling. Pumping on the helium to get below the lambda point is mandatory in order to avoid scattering of the infrared radiation by bubbles in the helium. The dewar requires over night precooling with liquid nitrogen before helium transfer if helium consumption is to be minimized. The additional set of windows in contact with the liquid helium can present some interference problems, particularly if the window coatings are not good. The major advantage of this technique is that one can be reasonably certain of the InSb surface temperature.

Cold finger operation is simpler once the initial difficulties are overcome. The cold finger in our apparatus is constructed of oxygen-free high-conductivity copper with about 2-3 mm thickness separating the liquid helium from the InSb resonator. Vapor deposition of gold[17] on one surface of the InSb appears to improve the indium solder bond between the sample and the cold finger. Our procedure is to precool the helium reservoir with liquid nitrogen then syphon this liquid to the nitrogen reservoir of the double dewar. This procedure reduces lead time for helium transfer to about 30 minutes. Cold finger operation is the obvious solution for operation with the resonator external to the InSb crystal. However, several undesireable effects may be present in this configuration. For instance, the output power may be less stable than in the immersed case. Also, if the input beam is chopped, the crystal can change temperature by larger amounts which can give rise to a frequency modulation, or chirping. To date, however, we have not observed these effects.

3. CARBON MONOXIDE PUMP LASER

An ideal pump laser for the spin flip laser would be one whose lines are separated by about 50 GHz, with several watts of power available on each line. Unfortunately such a laser has yet to be developed. The next best laser is perhaps the CO laser. The energy values for the $^{12}C^{16}O$ laser may be obtained from the following term value expression.[18]

$$
\begin{aligned}
T(v,J) = &\, \omega_e(v+\tfrac{1}{2}) - \omega_e X_e(v+\tfrac{1}{2})^2 + \omega_e Y_e(v+\tfrac{1}{2})^3 \\
&- \omega_e Z_e(v+\tfrac{1}{2})^4 + \omega_e a_e(v+\tfrac{1}{2})^5 - \omega_e b_e(v+\tfrac{1}{2})^6 + \cdots \\
&+ J(J+1)\left[B_e - \alpha_e(v+\tfrac{1}{2}) + \gamma_e(v+\tfrac{1}{2})^2 - \delta_e(v+\tfrac{1}{2})^3 + \cdots \right] \\
&- J^2(J+1)^2\left[D_e - \beta_e(v+\tfrac{1}{2}) + \Pi_e(v+\tfrac{1}{2})^2 - \cdots \right] \\
&+ J^3(J+1)^3\left[H_e - \eta_e(v+\tfrac{1}{2}) + \cdots \right]
\end{aligned}
$$

where the constants have the values, given in cm^{-1} as indicated below:

$$\omega_e = 2169.813\ 5802\,(881)$$

$$\omega_e X_e = 13.288\ 3076\,(435) \qquad\qquad B_e = 1.931\ 280\ 8724\,(443)$$

$$\omega_e Y_e = 1.05\ 1127\,(758) \times 10^{-2} \qquad \alpha_e = 1.750\ 441\ 21\,(729) \times 10^{-2}$$

$$\omega_e Z_e = -5.7440\,(541) \times 10^{-5} \qquad \gamma_e = 5.487\ 00\,(186) \times 10^{-7}$$

$$\omega_e a_e = 9.831\,(162) \times 10^{-7} \qquad\qquad \delta_e = 2.541\,(156) \times 10^{-8}$$

$$\omega_e b_e = 3.1660\,(173) \times 10^{-8} \qquad\qquad D_e = 6.121\ 468\,(291) \times 10^{-6}$$

$$\beta_e = 1.526(199) \times 10^{-9}$$

$$\Pi_e = 1.8050(154) \times 10^{-10}$$

$$H_e = 5.8272(597) \times 10^{-12}$$

$$\eta_e = 1.7375(229) \times 10^{-13}$$

The laser frequencies are the term differences

$$T(v + 1, J + 1) - T(v, J)$$

where v is the vibrational quantum number and J is the rotational quantum number. The resulting frequency differences between levels are indicated in Fig. 4 which points up the frequency spacing problem.

Since carbon monoxide lasers are not readily available commercially, we have constructed and used several lasers designed at NBS. We describe model II which is currently in use. This laser operates over a 1900-1700 cm^{-1} range and was designed for high output power at 6 μm to compensate for the fall off in resonance enhancement as one moves away from the band gap.

The resonator frame consists of 15 cm square aluminum end plates which are epoxied to 4 quartz rods, each 2 m long by 2.5 cm in diameter. One end plate holds a grating mount with an integral micrometer drive; the other end plate supports a mirror holder driven by a PZT piezoelectric stack or transducer. Adjustable irises at each end are used to force the laser to oscillate on a TEM_{oon} mode. Power is coupled out of the cavity through a 7mR, 90% reflectivity mirror. The second surface is flat and AR coated. The transmittance of the nominally 90% reflectivity mirror is shown in Fig. 6. The transducer can move the mirror about 10 μm. The sweepable drive voltage for the transducer comes from a standard NBS unit which was developed for laser stabilization. The drive unit has provisions for dithering, ramping, and servo correction. The other end of the resonator is terminated by an adjustable grating. We have
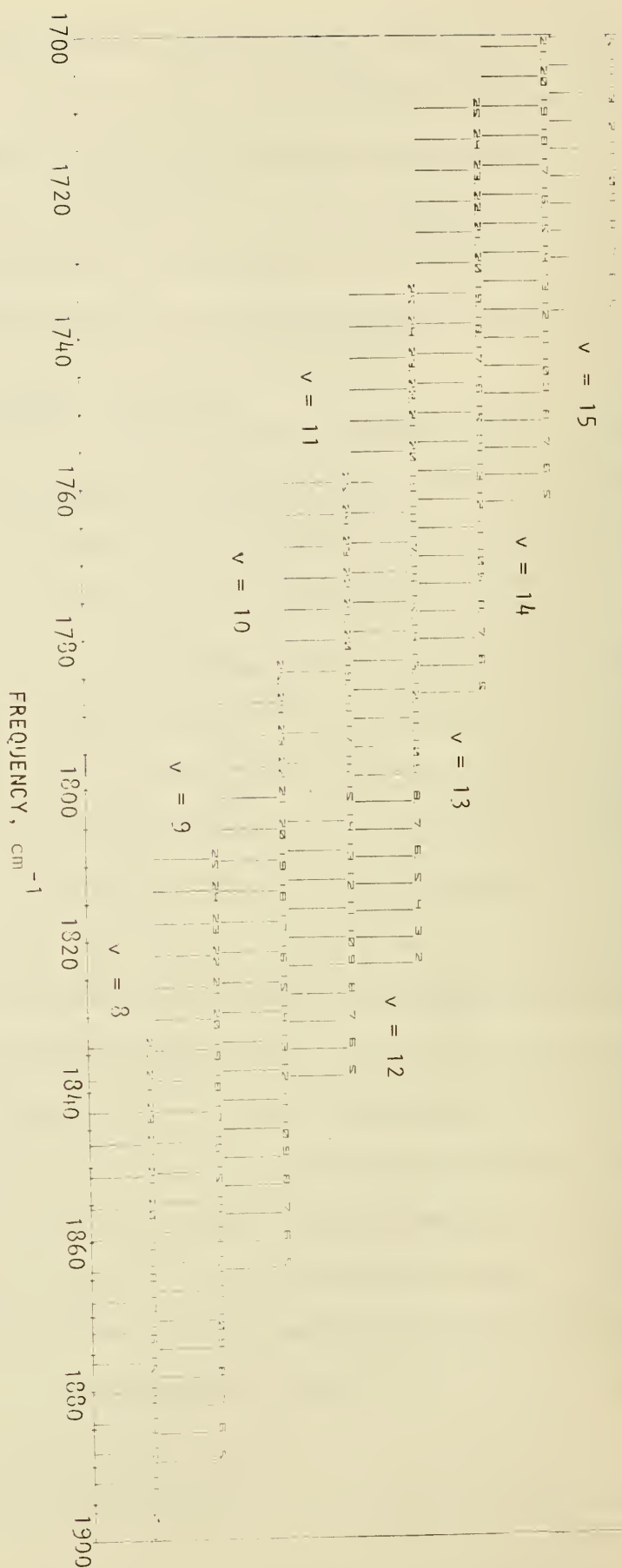
FREQUENCY, cm^{-1}

1700 · · · 1720 · · · 1740 · · · 1760 · · 1780 · · · 1800 · · 1820 · · · 1840 · · · 1860 · · · 1880 · · · 1900

v = 15   v = 14   v = 13   v = 12

v = 11   v = 10   v = 9   v = 8

Figure 4. Frequencies for CO laser between 1700 and 1900 cm^{-1}. These frequencies correspond to differences $T(v + 1, J + 1) - T(v, J)$. The vibrational quantum number v appears either to the left or right of the band. The transitions are all P transitions with the J value appearing above the frequency bar. Numerical values show that many of these transitions are very close to the same frequency. For instance, with our grating it is difficult to discriminate between $P_{12}(19)$ and $P_{11}(25)$. For this reason, not all of the transitions shown are suitable for pumping the spin flip laser.
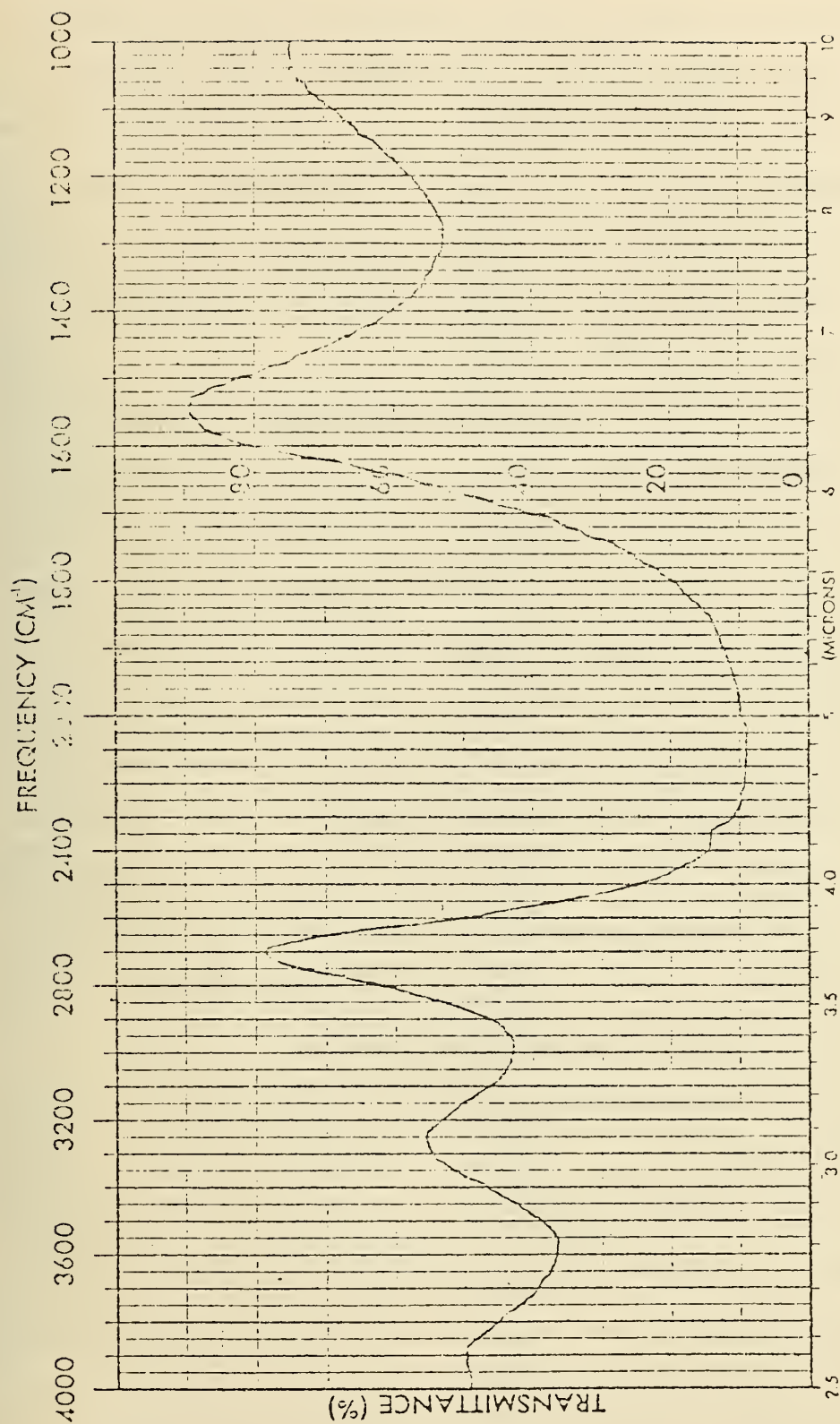
Figure 5. Transmittance of output mirror on carbon monoxide laser as a function at frequency and wavelength is shown above. The laser now operates between 5.2 and 5.8 μm. Operation can be extended to beyond 6.5 μm by choosing a mirror with higher reflectivity in the 6 μm region.

17

attempted to make a compromise between large dispersion and having a reasonable angle (the diffracted beam misses the rear output window for large angles) to permit use of the smaller power output from the grating. The particular grating in use has 240 groves/mm and a 26° 45' blaze angle. The relative efficiency for S polarization falls from about 95% to 5 μm to 90% at 6 μm for this model.[19] Table II shows the relative power output versus frequency for the CO lines which typically oscillate in this laser.

The 10 mm I.D. discharge tube is 192 cm long with Brewster windows at each end. Air spaces between the windows and resonator reflectors are sealed with bellows to avoid air currents in the optical path. The discharge is split with a single anode in the center and cathodes at each end to avoid undue heating due to ion bombardment which would result from the single cathode arrangement. All three electrodes are platinum "hollow cathode" elements.

A 30 mm O.D. concentric cooling jacket surrounds the discharge tube proper and a 4 mm ID tube which connects the discharge to a ballast region also allows communication from the anode to both cathodes. This connection is very beneficial in "sealed off" systems; otherwise, the power gradually diminishes during the course of the day due to impurity build up associated with cataphoresis. The connecting tube has stop cocks between the anode and each cathode to prevent the discharge from firing through the connection tube at start up. The discharge tube is shown in Fig. 5.

Two different cooling schemes are used. In both cases methyl-cyclohexane is used as the coolant. This coolant does not exhibit the viscosity of ethyl alcohol at reduced temperatures and does not freeze until 147 K. In one scheme, the methylcyclohexane is circulated through a heat exchange coil immersed in a mixture of dry ice and alcohol. A temperature of 203K can be maintained with

Table II

Multiline power output vs frequency for CO pump laser.

Grating micrometer reading in 0.001 cm	Operating frequency region in cm^{-1}	Power relative to maximum output
945	1915	.24
936.5	1911	.28
926.5	1906	.45
918.5	1902	.32
907.5	1898	.36
898	1894	.55
878	1884	.65
868.5	1880	.81
858.5	1876	.77
848	1872	.83
835	1867	.24
828.5	1863	.77
808.5	1855	.99
798	1851	1.00
788	1847	.76
777	1842	.73
763.5	1837	.26
757	1834	.73
744.5	1830	.26
736	1826	.44
724.5	1822	.86
714	1817	.55
709.5	1813	.72
692	1809	.75
680.5	1805	.46
669	1801	.45
636	1788	.53
625	1784	.60
615	1780	.34
600	1776	.36
579	1767	.47
568.5	1763	.49
556.5	1759	.43
545	1755	.44
530	1751	.34
520	1747	.19
508	1743	.34
496	1738	.37
480	1733	.10
469	1729	.24
456.5	1726	.28
445	1722	.26
421	1714	.18
404	1709	.14

CO LASER DISCHARGE TUBE

CATHODE

NaCl WINDOW AT
BREWSTERS ANGLE

8mm OD

COOLANT OUTLET

COOLING JACKET

CONNECTING TUBE

91.5cm

4.5cm

BALLAST RESERVOIR

STOPCOCKS

#18 BALL
JOINT

30mm OD

ANODE

12mm OD

6mm OD

51mm OD

ELECTRODE SUPPORTS 90° FROM
PLANE OF CONNECTING TUBE

W ROD, 1.5mm DIA

19mm OD

PT THIMBLE, 12.7mm OD,
0.4mm WALL, 30mm LONG
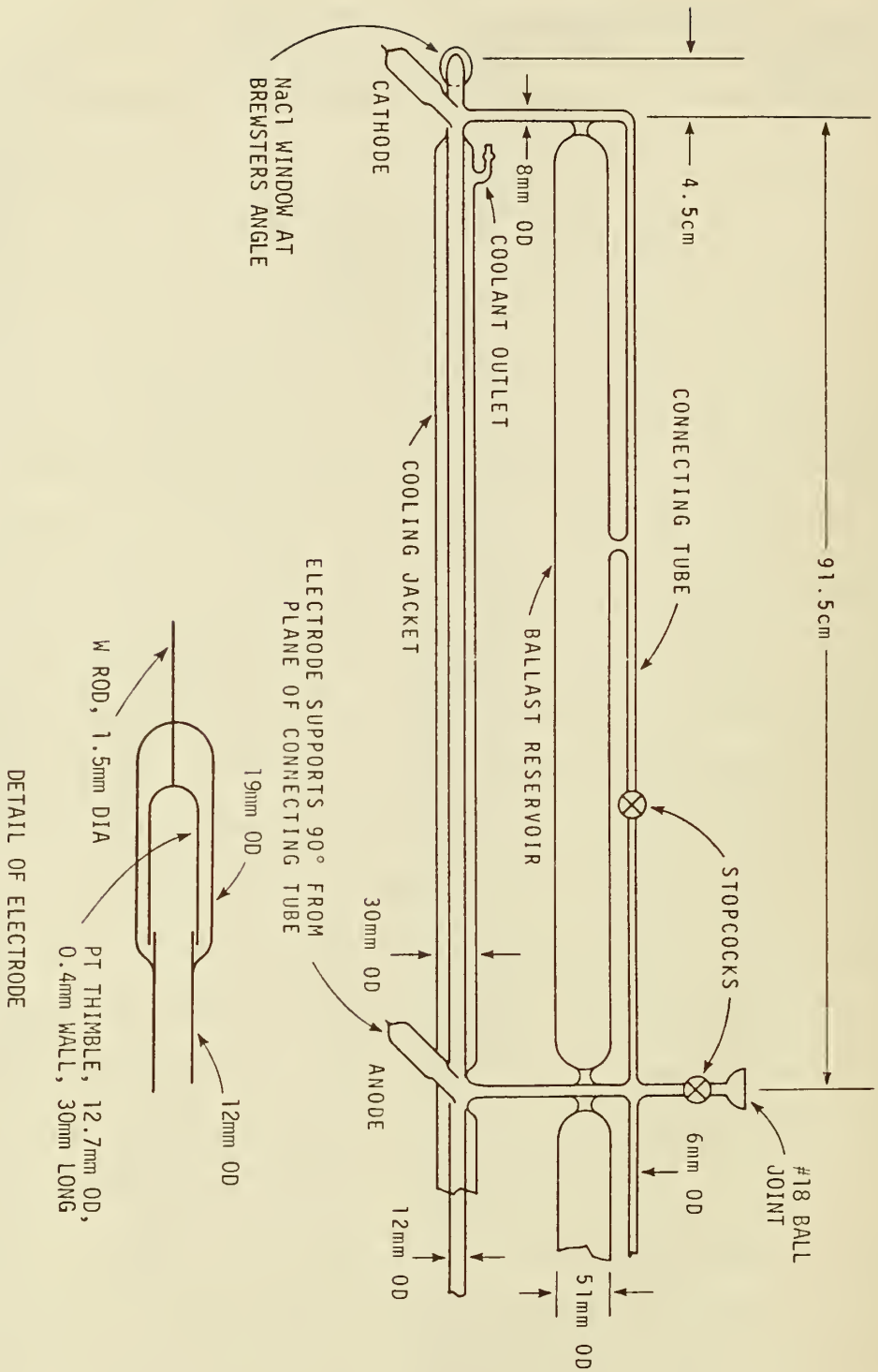
12mm OD

DETAIL OF ELECTRODE

Figure 6. Sketch of CO pump laser discharge tube design. Overall tube length is 192 cm and the tube is symmetric about the anode plane, except for coolant inlet which comes in at the bottom of the cooling jacket.

20

this arrangement. At laser operation near 6 μm, however, lower temperatures are required and a second cooling coil in series with the first is immersed in a methylcyclohexane bath. Liquid nitrogen flowing through an additional coil in this bath cools the methylcyclohexane to near its freezing point. With this system, a temperature of 158°K can be attained. This second stage is bypassed for 5.3-5.5 μm operation.

The gas fill mixture in the CO laser[20] is a premix of 6.3% Xenon, 6.3% nitrogen, 6.3% carbon monoxide and the balance is helium. Typical fill pressures vary between 2,000 and 2,700 Pa (15 and 20 Torr), depending on the intended operating temperature. The discharge current is typically around 10mA. Each side of discharge is powered by a 25 kv power supply with 200 k ohms of ballast resistance in the circuit.

The transducer controlled mirror permits one to adjust the frequency of the CO laser within its gain profile. A reference frequency is synthesized by a method described in the next section. The CO laser frequency is locked 30 MHz away from this reference frequency by means of a 30 MHz discriminator, an operational amplifier and filter, and the previously mentioned driver unit which adds the amplified correction voltage to the bias voltage already on the PZT transducer.

4. INFRARED FREQUENCY SYNTHESIS TECHNIQUES

One of the prime objectives of the infrared frequency synthesis (IFS) program at the National Bureau of Standards (NBS), was to determine the frequency of the 3.39 μm P(7) transition in methane. In the process of achieving this goal, two definitive CO_2 laser frequency measurements were made.[3] Using these two frequencies as a basis, a thorough program to determine values for stabilized CO_2 laser frequencies was undertaken and completed at NBS.[4] By using two CO_2 lasers, a klystron, and an appropriate diode one may synthesize any frequency between 0 and 100 THz.[21] A list of two-laser, CO_2 combinations for generating frequencies in this fashion has been compiled. More recently, the IFS technique has been used to measure the frequency of the Xenon laser at 2.0 μm.[22] A long term objective has been to extend the technique to the visible. A secondary objective is to laterally extend the technique to use the CO_2 laser synthesizer with tunable lasers and make absolute frequency measurements.

An example of two-laser infrared frequency synthesis is shown in Fig. 7. To accurately measure the frequency of a laser, ν_M, a frequency, ν_s, which is close to the frequency to be measured, must be synthesized. The difference between these two frequencies is an intermediate frequency, ν_{IF}, typically less than one GHz. The unknown laser frequency is:

$$\nu_M = \nu_s \pm \nu_{IF}$$

$$\nu_s = \ell\nu_1 + m\nu_2 + n\nu_{\mu W}.$$

ν_1 and ν_2 are basis laser frequencies which have been determined by prior synthesis measurements, and $\nu_{\mu W}$ is a microwave frequency. The quantities
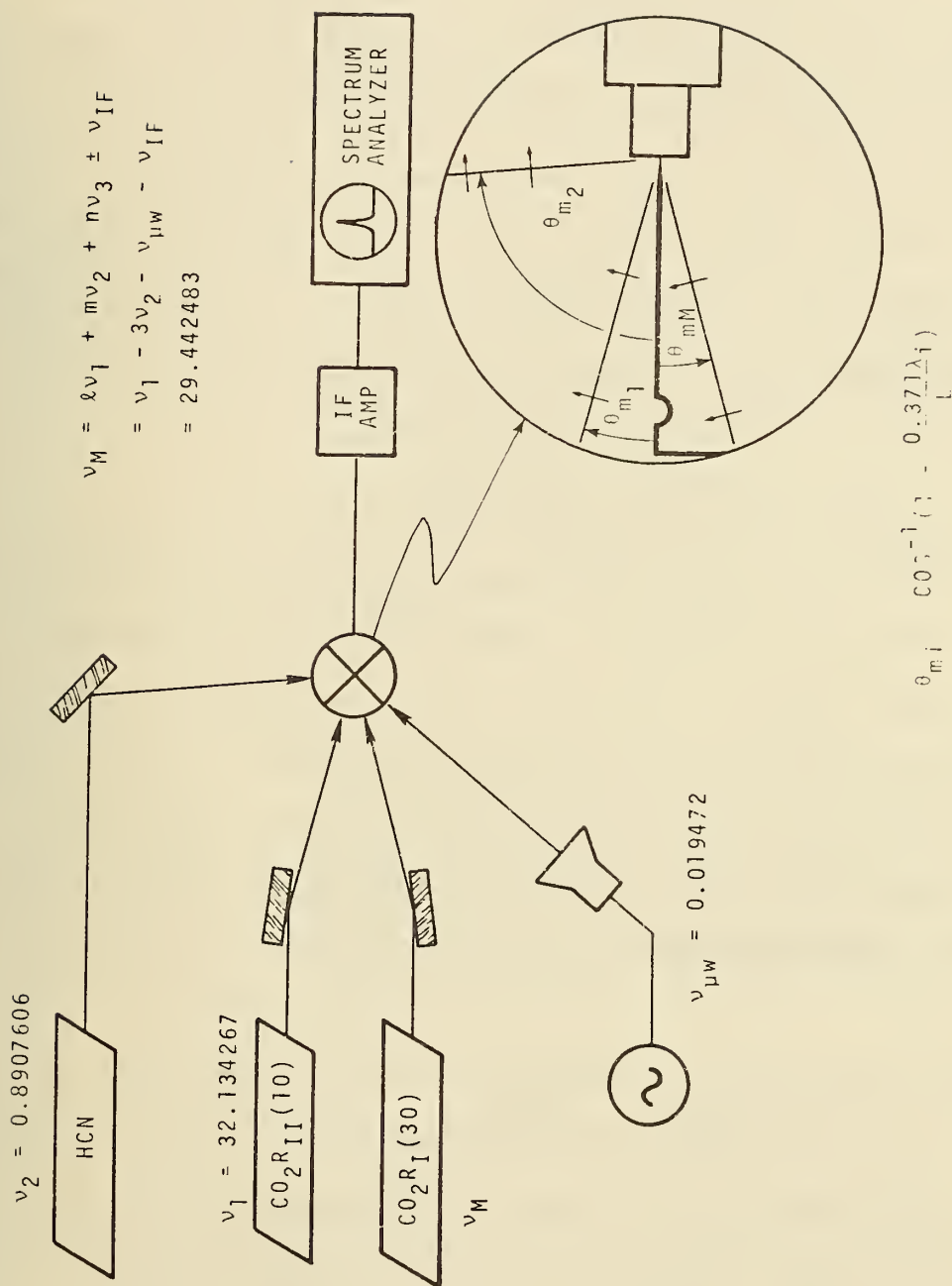
Figure 7. Example of infrared frequency synthesis. All frequencies are given in terahertz (THz). The signal from the IF amplifier may be used for frequency measurement and, or control.

$\nu_2 = 0.8907606$

HCN

$\nu_1 = 32.134267$

$CO_2R_{II}(10)$

$CO_2R_I(30)$

ν_M

$\nu_{\mu w} = 0.019472$

$\nu_M = \ell\nu_1 + m\nu_2 + n\nu_3 \pm \nu_{IF}$

$= \nu_1 - 3\nu_2 - \nu_{\mu w} - \nu_{IF}$

$= 29.442483$

IF AMP

SPECTRUM ANALYZER

θ_{m2}

θ_{mM}

θ_{m1}

$\theta_{mi} \quad \cos^{-1}(i \cdot - \dfrac{0.371\lambda_i}{L})$

23

ℓ, m, and n are harmonic numbers which are allowed both positive and negative values. The quantity $(1 + |\ell| + |m| + |n|)$ is called the mixing order.[23] The harmonic generation as well as the mixing which produces the intermediate frequency to be measured, occurs in a suitable diode, typically a tungsten catwhisker on a nickel base.[24,25] Two relevant points are indicated in Fig. 7. First, the laser beams are polarized with the electric field vector in a plane which contains the catwhisker antenna. Second, the angles between the laser beams and antenna are given by long-wire antenna theory.[26] According to this theory, the angle between the antenna direction and the direction of the first maximum in the radiation pattern is given by

$$\theta_{max} = \cos^{-1}\left(1 - \frac{0.371\lambda}{L} \right)$$

where λ is the wavelength of the radiation being coupled to the antenna and L is the distance between the tip of the tungsten wire and some discontinuity in the wire, either in shape or direction. Although some contention exists as to the type of coupling that prevails at 3.39 μm (perhaps a conical antenna)[3] our experiments indicate that the long wire antenna theory is applicable at 5.3 μm. Our measured value of $\theta_m = 11^{\circ} \pm 1^{\circ}$ is commensurate with the antenna length at 100 μm. The unetched diameter of the antennas used in this work is 25 μm.

The physical mechanism of the harmonic generation in these diodes is not universally agreed upon. Theories postulating asymmetric tunnelling due to geometry, quantum mechanical scattering, field emission, and barrier tunnelling have been made. In some of the tunnelling theories voltage is considered the independent variable; in others the current appears as the wave fundamental quantity. Since the antenna coupling tends to be associated

24

with generation of currents and the existence of currents near 10^{14} Hz

has been demonstrated, this latter theory has considerable appeal.

The essential ideas of one tunnelling theory[27] are as follows.

The diode consists of two dissimilar metals (nickel and tungsten in our

case) separated by some unspecified insulating barrier, probably an oxide

which is several lattice parameters thick. If $\emptyset_1$ and $\emptyset_2$ are the work

functions for metals one and two and V is the voltage between the two

metals, the expressions for the electron tunnelling currents given by

Simmons[28] are:

$$I_f = \frac{Ae}{2\pi ht^2} \left[\emptyset_2 e^{-T\emptyset^{\frac{1}{2}}} - (\emptyset_2 + eV) e^{-T(\emptyset_2 + eV)^{\frac{1}{2}}} \right]$$

for $V > 0$ and

$$I_r = \frac{-Ae}{2\pi ht^2} \left[\emptyset_1 e^{-T\emptyset_1^{\frac{1}{2}}} - (\emptyset_1 - eV) e^{-T(\emptyset_1 - eV)^{\frac{1}{2}}} \right]$$

for $V < 0$

The quantity A is the contact area of the diode, which may correspond

to a 500 - 100 Å radius of the tip, and t is the approximate barrier thickness,

15 - 20 Å. T is given by

$$T = \frac{4\pi(t_2 - t_1)}{h} \sqrt{2m_e} \approx \frac{4\pi t}{h} \sqrt{2m_e}$$

where t_2 and t_1 are classical turning points in the barrier penetration

problem. The quantities e, m_e and h are the electron charge, electron mass

and Planck's constant, respectively. While no further use of the above expressions

is made here, they do show one explicit current-voltage relation and indicate some

dependence of the current on the. physical dimensions of the junction of the diode.

25

It is then assumed that the current, I, through the diode consists of an external bias, i_b, plus currents which the laser radiation induces in the antennas. For example,

$$I = i_b + i_1 \cos\omega_1 t + i_2 \cos\omega_2 t$$

This current and the tunnelling current expressions are combined to give the voltage as a function of current

$$V = g(I)$$

where $g(I)$ is a non-linear function of the total current.

The harmonic generation is mathamatically evident when $g(I)$ is expanded in a Taylor series about the bias current, i_b.

$$V = g(i_b) + \frac{dg}{dI}\bigg)_{i_b} (i_1 \cos\omega_1 t + i_2 \cos\omega_2 t)$$

$$+ \frac{1}{2!} \frac{d^2 g}{dI^2}\bigg)_{i_b} (i_1 \cos\omega_1 t + i_2 \cos\omega_2 t)^2 + \ldots$$

The general term corresponding to the nth harmonic has not been shown since we can illustrate our immediate use with the second order term. For stabilization of the CO laser, we have not found it necessary to use an external biasing current on the diode; hence i_b equals zero. An examination the second order term indicates constant terms proportional to i_1^2 and i_2^2 as well as terms involving sum, difference, and doubled frequencies. These constant terms represent rectified optical signals and can be used to advantage to monitor coupling of a particular radiation to the diode. This is accomplished by chopping the laser radiation and adjusting the optics for a maximum value of the modulated rectified voltages on an oscilliscope, (typically indicated in Fig. 8), which shows rectified signals and the resulting beat notes.
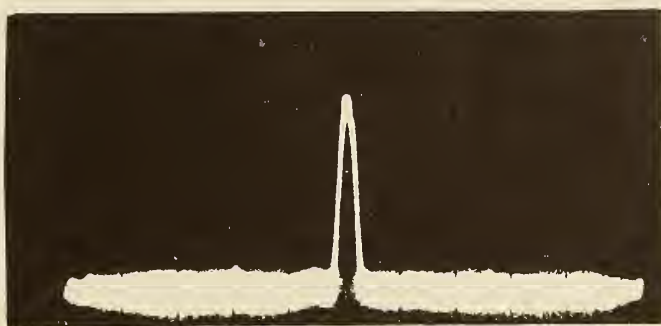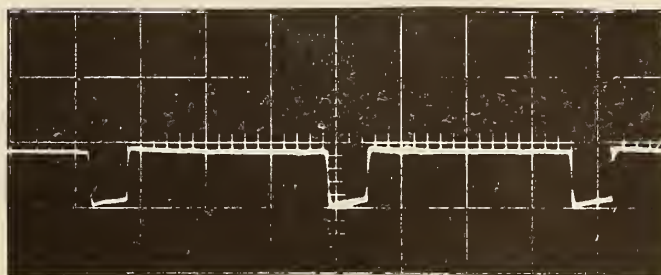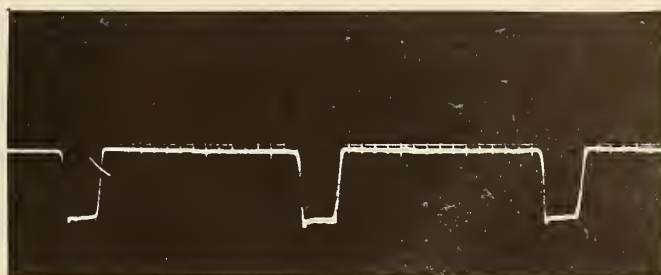
Figure 8. Rectified voltages for CO_2 and CO lasers on a metal oxide metal diode. a) Rectified CO_2 induced voltage on a 5 mV per division scale. b) Rectified CO induced signal on a 0.5 mV scale. c) Beat note at 30 MHz when a 46 GHz signal from a klystron additionally irradiated the diode. Signal to noise ratio for the beat note is 30 db and dispersion is 1 MHz/division. The spectrum analyzer bandwidth is 100 kHz and sweep time is 1 ms per division.

27

The coefficients of the frequency sum and difference terms are proportional to the product of the two laser induced current amplitudes. Thus, by compensating with increased power from one laser, mixing experiments can be done even though the other laser induced signal may be weak. Significant non-linearities, such as burning-up of the tungsten antenna, will ultimately limit the extrapolation of this technique. Hopefully, power compensation by one of the synthesis lasers may help solve the problem of measuring the frequency of the relatively low power, spin-flip laser. We defer that discussion until the latter part of this section.

In order to see the desireability for IFS techniques with the stabilized CO_2 lasers in our spectrometer, we need only consider some of the properties of CO and CO_2 lasers.

The CO_2 laser is unique in that it has over 100 lines (more or less uniformly spaced) extending from 9 to 11 μm, all of which can be stabilized to standing-wave saturation resonances observed in the 4.3 μm fluorescent radiation. The fractional frequency variation of lasers stabilized in this way at the National Bureau of Standards[4] is $3 \times 10^{-11} \tau^{-\frac{1}{2}}$ for $10^{-2} \leq \tau \geq 10s$. It is estimated that the fractional uncertainty in the resetability of each CO_2 laser is about 2×10^{-10}. Further, the absolute frequencies of these lines are known to within about one part in 10^9.

The lines in the CO laser do not have the same desirable separation as in CO_2; in fact many transitions nearly overlap, and unfortunately the CO_2 stabilization technique cannot be used for CO. We have used an alternative stabilization procedure for CO, as shown in Fig. 1. Here the CO laser is locked to a frequency which has been synthesized from the second harmonic of a stabilized CO_2 laser and an appropriate microwave frequency. Both the 2nd harmonic generation and the mixing are done simultaneously in the point

contact diode with the properties indicated in the caption of Fig. 8. Over 100 CO lines lie within 40 GHz of the second harmonic of some CO_2 laser line and may be stabilized in this manner. The CO laser would then have nearly the same long term stability as CO_2, and its absolute frequency would be known to within a part in 10^9. This procedure increases the utility of the CO laser as a pump for a tunable Raman spin flip laser to be used for high resolution spectroscopy. Also, as a monitor of the CO laser operation, one can observe the output from the diode and make appropriate adjustments to insure that the CO laser is operating in a single mode and on a single transition.

The problem of measuring the difference frequency between the pump laser and the SFRL output is complicated by three factors. First, the spin flip and pump signals have mutually orthogonal polarizations, which originally presented difficulties in coupling to the diode antenna. Second, the power output from the SFRL is low compared to levels generally used for synthesis in MOM diodes. Third, the large colinearly-transmitted pump power makes focusing the weak SFRL output beam on the diode difficult.

Long wire antenna theory indicates that for best coupling the antenna should be rotated in the plane of polarization by the angle Θ_m with respect to the beam direction. Normally, our diode holders have provision for rotation in the horizontal plane only. A tapered fixture which tips the diode down 11° in the vertical plane while maintaining an 11° projection in the horizontal plane with respect to the beam direction has permitted 5 μm signals with either polarization to be coupled to the diode.

An InSb crystal with an electron concentration around 4×10^{15} cm^{-3} has a maximum in the power output curve at about 0.2 Tesla as indicated in Fig. 3. We have used a crystal with a carrier concentration of 2.5×10^{15}

29

cm^{-3} and obtained an estimated 30 mw maximum output power near 0.205 Tesla.
This point of operation is selected since the frequency difference between
the CO pump and the SFRL is predicted to be about 150 GHz corresponding to
the 2nd harmonic of an available klystron. Since the power available from
the SFRL is low, it is deemed desirable to keep the mixing order as low
as possible in the initial experiments. The SFRL power density is increased
at the diode junction by focusing it down with a 2.5 cm focal length lens.
Sufficient transmitted pump power (although the radii of curvature of the
pump and SFRL signals are not generally equal) might also be coupled to the diode
through the same lens to produce a beat note between the laser and the
75 GHz klystron. We are exploring the possibility of measuring the frequency
difference in this manner.

    While the MOM diode has considerable potential for heterodyning the
SFRL signal, a reliable procedure needs to be developed for coupling the
laser signal to the diode. Some of this development involves improvements
in the SFRL itself. An external resonator configuration would permit
single mode operation of the SFRL, a single wave front for coupling to the
diode, and hopefully greater power output. The inclusion of a Brewster angle
window within the resonator could also reflect some of the troublesome
transmitted pump radiation from the beam. An additional improvement would
be to bring the pump and spin flip beam to the diode along separate path
lengths as proposed in Fig. 17, for example. Separate focusing would afford
some control over the relative powers, permit parameters to be evaluated
on a quantative basis, and pave the way for routine heterodyning procedures.

5. OPTO-ACOUSTIC DETECTOR

The development of air pollution monitoring equipment capable of detecting the presence of atmospheric trace constituents at concentrations as low as one part per billion has led to a number of highly sensitive measurement techniques. One such device developed on our laboratory and elsewhere is the resonant opto-acoustic detector.

In this device a confined gas is irradiated by a laser tuned to a vibrational frequency of the molecules in the gas, and consequently, some of the gas molecules reach an excited state. Subsequent collisional de-excitation of these molecules results in a thermalization of the absorbed energy and therefore a pressure rise in the gas. Thus, modulation of the intensity of the irradiating laser produces pressure fluctuations which may be detected by a suitably mounted microphone. If, in addition, the laser is modulated at a frequency which corresponds to one of the natural acoustic resonances of the gas confining cavity, the acoustic signal generated will be enhanced by an amount proportional to the cavity Q, thus, greatly increasing the system sensitivity. The basic features of such a system are illustrated schematically in Fig. 9 (details available elsewhere)[5] which shows a cylindrical sample cavity with a microphone mounted flush with the cylindrical wall. In addition, Fig. 9 indicates that we have greatly enhanced the chance for absorption of the irradiating laser beam by multiply reflecting it between two mirrors forming the end walls of the cavity, thus further increasing the system detection sensitivity.

Measurements with this system have demonstrated acoustic Q's exceeding 750 and detection linearity for all absorber gas concentrations below a saturation threshold which corresponds roughly to an absorption coefficient of 6×10^{-2} cm^{-1}. Since the opto-acoustic detection sensitivity is directly proportional to the absorbed infrared energy, direct comparison with conven-
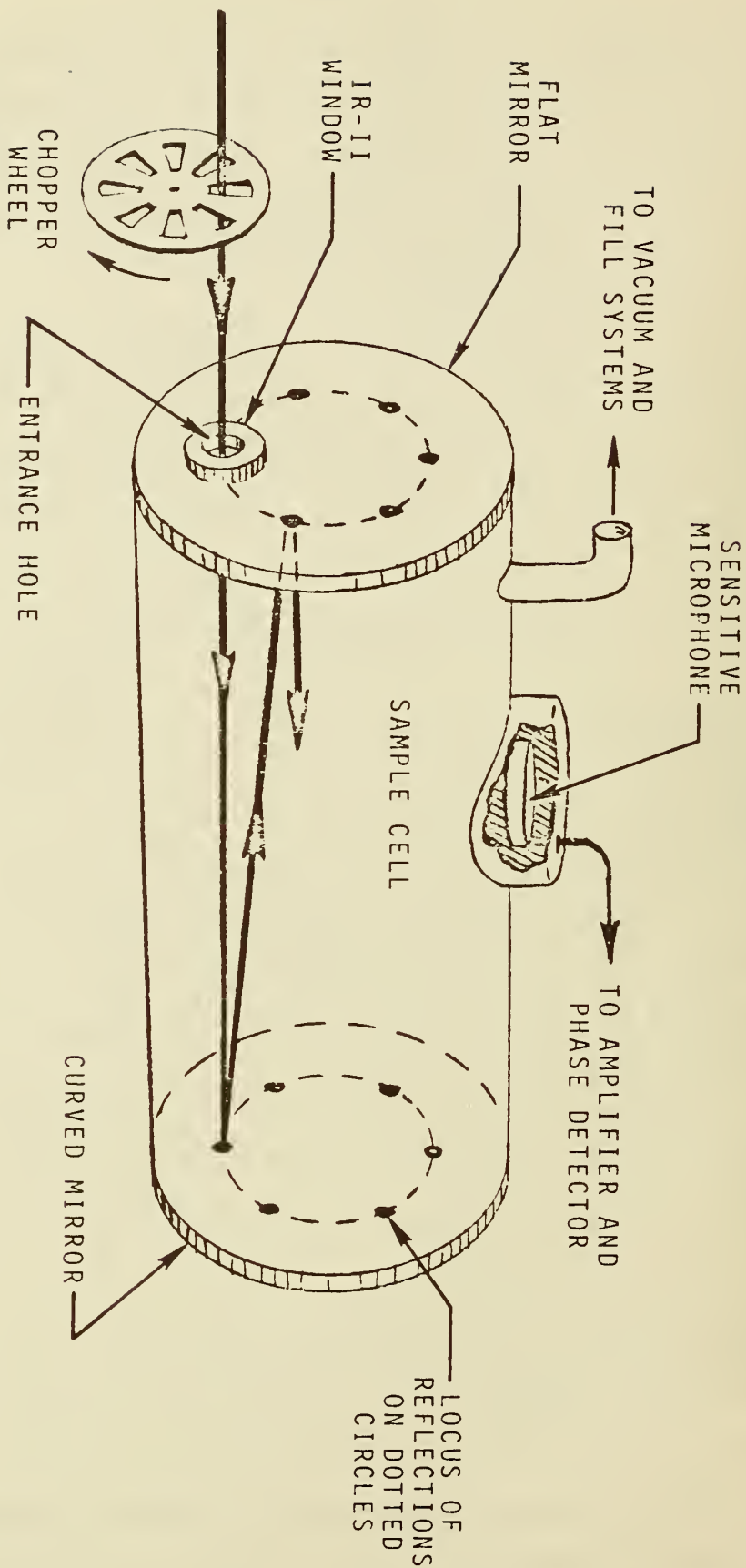
31

OPTO-ACOUSTIC DETECTOR

FLAT
MIRROR

IR-II
WINDOW

CHOPPER
WHEEL

ENTRANCE HOLE

TO VACUUM AND
FILL SYSTEMS

SENSITIVE
MICROPHONE

SAMPLE CELL

TO AMPLIFIER AND
PHASE DETECTOR

CURVED MIRROR

LOCUS OF
REFLECTIONS
ON DOTTED
CIRCLES

Figure 9.   Schematic drawing of opto-acoustic detector incorporating multiple pass system.
The incident laser beam undergoes multiple reflections centered on the locus of
reflection circle, due to the mirror arrangement selected.   The cell has success-
fully operated at pressures as low as 700 Pa (5 Torr) and should be useful to
measure spectra of compounds with low vapor pressure.

tional measurement techniques which depend only upon fractional absorption is somewhat difficult. Measurements to date indicate, however, that a signal to noise ratio of 1 is achieved at a bandwidth of 1 Hz, with a 1 watt irradiating laser and a gas fill having an absorption coefficient of 3×10^{-9} cm^{-1} at 53,000 Pa (400 Torr). To achieve comparable sensitivity, a conventional absorption detection system would require an effective absorption path length of ~100 meters compared to the 20 cm opto-acoustic absorption cell.

The opto-acoustic system thus currently displays a linear detection range exceeding 7 orders of magnitude. The system noise is currently dominated by electronic amplifier noise whereas the fundamental limitation is the thermal acoustic noise on the microphone element itself. Improvements in microphone and electronic design should allow us to reach this fundamental limitation. Improvements in the cavity optical design should also result in greater system ultimate sensitivity.

Since the detection system requires the conversion from vibrational excitation to random thermal energy via a gas kinetic collision mechanism, some loss in system sensitivity is bound to occur as the cell pressure and thus the molecular collision frequency is reduced. We have, however, made relatively low level absorbtion measurements at pressures as low as 700 Pa (5 Torr) indicating that measurements even at low pressures may be made by the opto-acoustic technique. More work in this area is needed to see if specialized microphone design could improve the low pressure measurement capabilities. A device such as this offers advantages on two counts. One, materials having low vapor pressure at room temperatures could be investigated and two, particulate scattering (which could be a problem in transmission spectroscopy) does not adversely affect operation. A spectrum obtained by using the opto-acoustic detector and spin flip laser is shown in the next section.

6. ENVIRONMENTAL PROBLEMS

The spin flip laser (including the CO pump), opto-acoustic detector, a stabilized CO_2 laser, and some additional infrared frequency synthesis apparatus are assembled into the system shown in Fig. 10.

A stabilized CO_2 laser, microwave source, and point contact diode are used to synthesize a suitable reference to frequency offset lock the CO laser. For example, P(17) in the 8 to 7 band for the CO laser is stabilized by operating the CO_2 laser on P(18) in the 10.6 μm band and phase locking the microwave oscillator to 46.608 GHz. When these three oscillators simultaneously irradiate the diode, a 30 MHz beat note is produced which is used to stabilize the CO laser frequency. The correction voltage generated by a conventional discriminator is amplified and applied to a piezoelectric transducer on the CO laser. Stabilization of other CO laser lines requires additional klystrons.

A reference oscillator and power amplifier control the speed of the synchronous motor which drives the chopper. The chopping at the opto-acoustic detector frequency is done preceeding the InSb sample to minimize heating of the crystal in the cold finger configuration. The beam from a light-emitting diode is also chopped, and this signal provides the reference for the phase detector.

The signal from the opto-acoustic detector is also fed to a phase detector, and its output is fed to the Y-axis of an X-Y recorder. The X-axis is driven by a signal derived from a Hall probe in the magnet.

In an alternate simple absorption experiment, a mirror is used to direct the spin flip output through a 10-cm-long absorption cell equipped with Brewster windows. The filter may be a monochromator, and the detector currently in use is a gold-doped germanium diode.
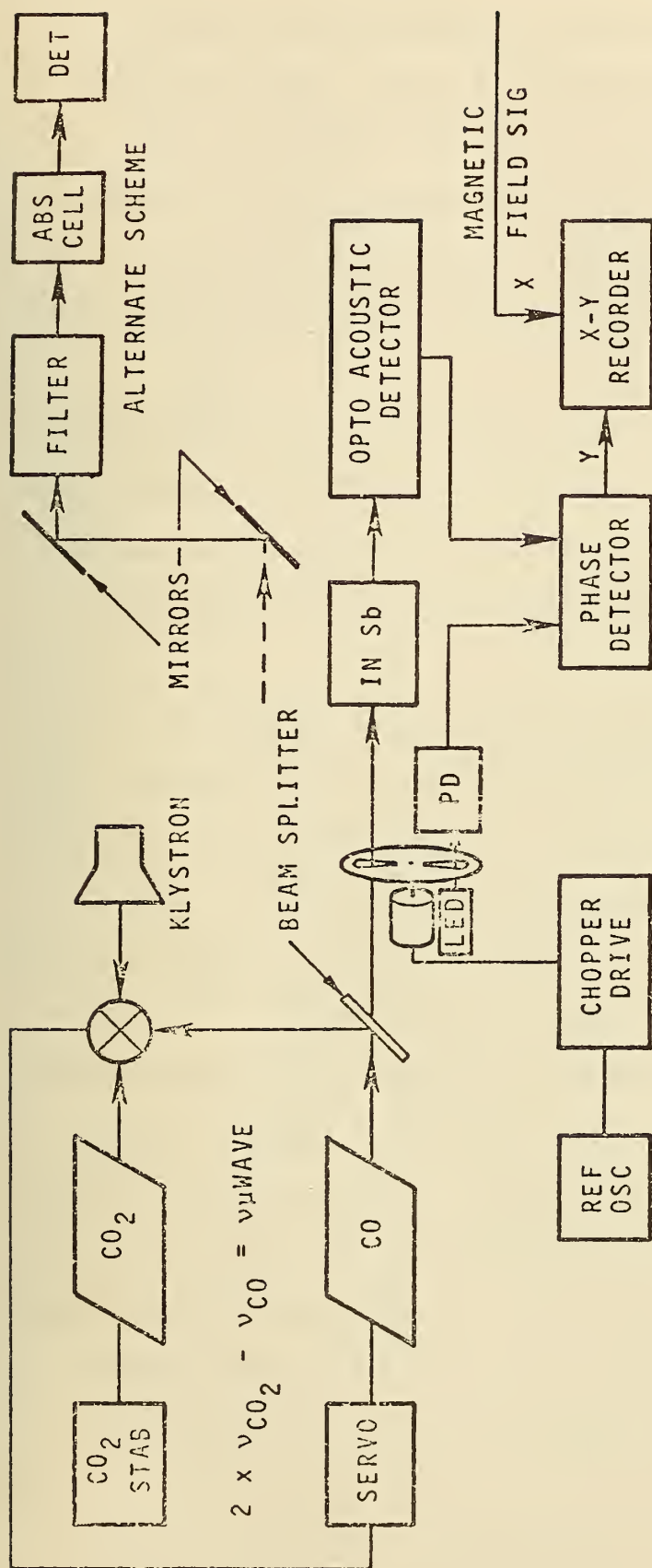
Figure 10. Block diagram of spectrometer employing spin flip laser, CO_2 laser standard and opto acoustic detector. The frequency of the CO laser is stabilized by locking it to a reference synthesized from a CO_2 laser in a metal oxide metal diode. The CO pump beam is chopped at the acoustic resonance frequency of the opto acoustic detector. The chopper along with a light emitting diode and photo detector provide a reference for the phase detector. The cryogenic apparatus and magnet which were shown in Fig. 1 have been omitted from this diagram.

The application of the first scheme to detection of pollutants is demonstrated by the nitric oxide spectrum in Fig. 11. Nitric oxide[29] has a large number of strong lines within the frequency capability of the system. Tunability of the spin flip laser permits selection of a transition which avoids the spectral lines of other pollutants. By tuning the laser to the $R(\frac{1}{2})$ transition, a sensitivity of one part in 10^{-7} of NO can be achieved with a 30 mW SF signal.

The operating pressures in the opto-acoustic cell (about 6,700-53,300 Pa or 50-400 Torr of buffer gas) so far have precluded high-resolution non-pressure-broadened spectroscopy. However the spin flip laser does have this capability. This resolution is demonstrated in Fig. 12 where the alternate system has been put into use.

The system is not limited to use for detection or identification of pollutants which have a fundamental band overlaping the 5.3 μm region. For example several molecules have overtone bands which also fall within this region. As an example, the spectrum of SO_2 is shown in Fig. 13. This characteristic signature of SO_2 in this region provides an interesting contrast with the simple and well known spectra of NO in Fig. 11.

Finally we point out the potential for chemical kinetics investigations in this region. Due to the great selectivity and high sensitivity for molecular detection achieved with the tunable IR radiation of the SF laser, this system should prove excellent for chemical kinetics studies. Once an appropriate spectral feature has been chosen, it can be monitored quantitatively throughout the reaction providing the frequency of the SF signal does not change. This is assured by the frequency locking servo on the CO laser
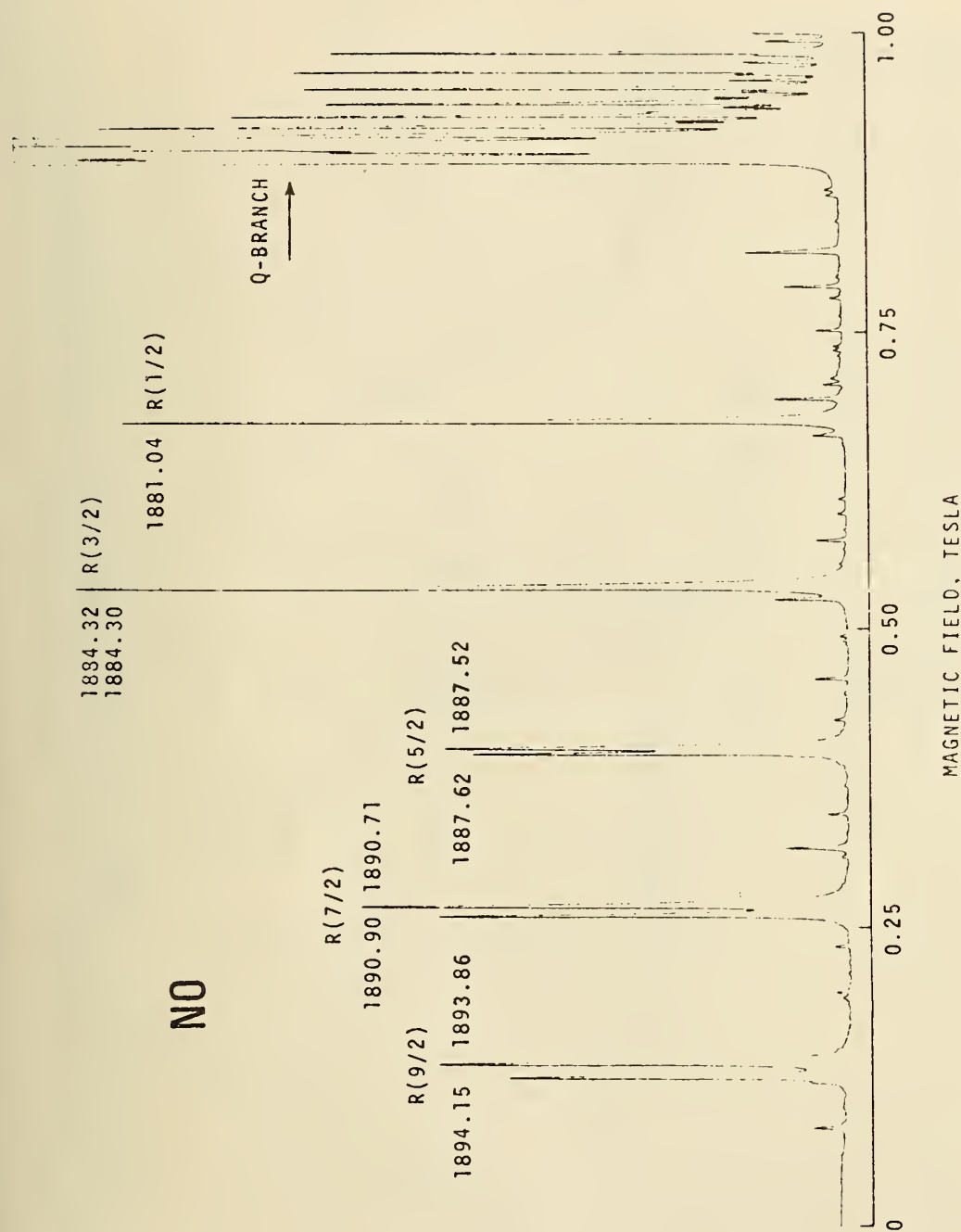
Figure 11. Absorption spectrum of 0.02% nitric oxide in 6,700 Pa (50 Torr) of nitrogen gas in the opto acoustic detector. The spin flip laser was pumped at 1897.66 cm^{-1} and the magnetic field sweep was 1 Tesla. Both $^2\Pi_{3/2}$ and $^2\Pi_{\frac{1}{2}}$ transitions are resolved for R(9/2) at 1894 cm^{-1}, R(7/2) at 1891 cm^{-1} and R(5/2) at 1888 cm^{-1}. Q-branch transitions appear starting about 1876 cm^{-1}.
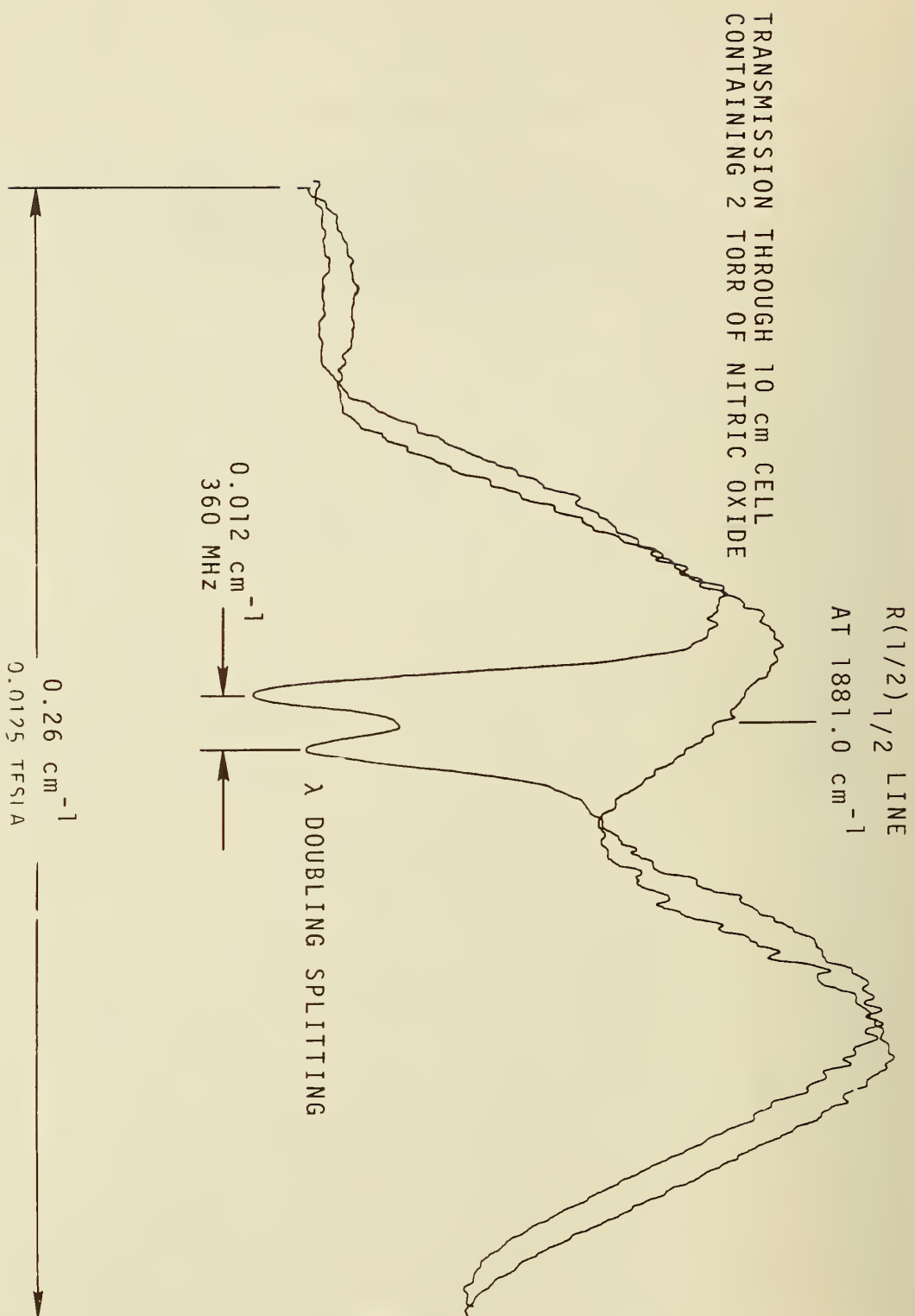
Figure 12. Spectrum of R(1/2) 1/2 transition in NO obtained at NBS-ilOAA with spin flip laser and gold doped germanium detector. One trace is with the 10 cm long absorption cell empty, the second shows the transmission with 300 Pa (2 Torr) of NO in the cell. The λ doubling is clearly resolved, indicating a resolution around 0.01 cm^{-1}.
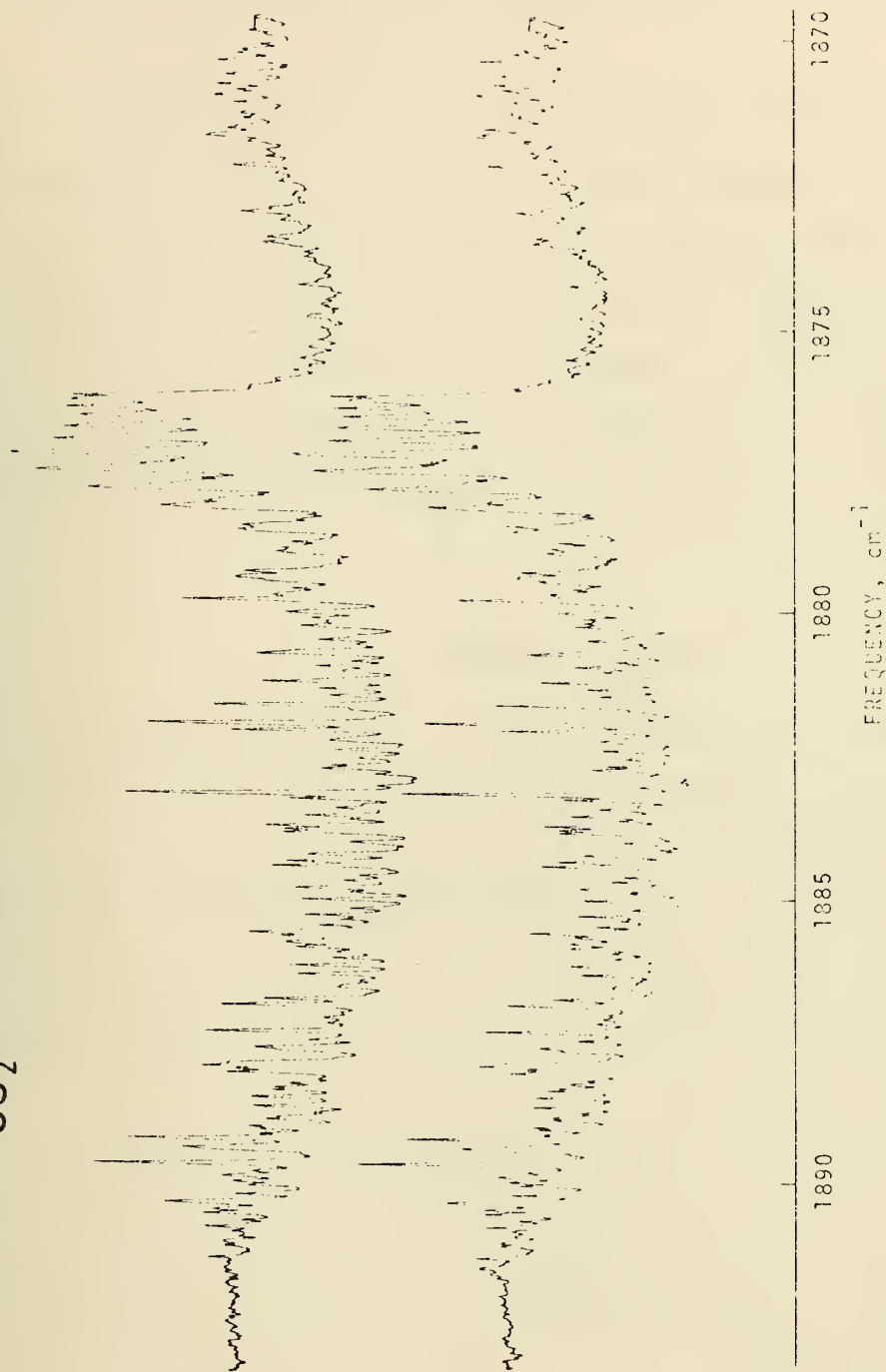
Figure 13. Spectrum of 1% SO_2 in 13,300 Pa (100 Torr) N_2 mixture in opto acoustic detector. Spin flip laser was pumped at 1893 cm^{-1}. Magnetic field sweep is 1 Tesla. Two runs are shown to better distinguish signal from noise. The spectrum is due to overtone bands in the SO_2 molecule.

39

and the feedback control which maintains the magnetic field at a constant value.

Either the opto-acoustic detector or the simple absorption cell may be used to monitor the gas concentration in a flow tube system.[30] The opto-acoustic detector, however, unless modified to obtain low turbulence flow characteristics, is suitable only for very low flow velocities and hence measurement of slow reactions. Because of this constraint, a flow tube system incorporating an absorption cell is currently under construction to study kinetics of some of the free radicals detectable within the available tuning range of the SF laser.

7. METROLOGY PROBLEMS

Most of the technological problems that the spectrometer could help solve would involve making absolute frequency measurements. One category would be to provide reference or bench mark frequencies that diode laser users could find beneficial. Diode lasers at present do not have sufficient power to use with metal-oxide-metal diodes, and while they do afford excellent potential for high resolution,[31] they apparently are not exactly reproducible from day to day in regard to their frequency-current relations. Large facilities where diodes are in use are forced to refer all measurements to an internal standard whose absolute frequency is not known.[32] Fig. 14 indicates the type of spectrum that could be useful as a reference in regions where the spin flip laser operates.

A second category of experiments is related to some current activities regarding isotope separation and a related class of two-photon experiments[33] involving CO_2 lasers. Since the CO_2 laser has very desireable properties,

Figure 14. Absorption spectrum of 1,300 Pa (10 Torr) of H_2O in 38,700 Pa (290 Torr) N_2 gas mixture in the opto acoustic detector. The spin flip laser was pumped at 1893 cm^{-1} and the magnetic field was swept 1 Tesla. The strong transition at 1889 cm^{-1} (relative intensities are perturbed due to the weakness of spin flip output at onset of oscillations here) has been used by Patel in a saturated absorption experiment. The apparent structure of the 1889 line is due to fluctuations of the spin flip laser power which occur near threshhold for stimulated operation. The lines in the quartet at 1880 cm^{-1} have the narrowest linewidths of any water vapor lines yet studied and should be useful for a frequency reference.

41

such as high efficiency, high power, cleanly separated transition frequencies and scaleability, several proposals have been put forth to use CO_2 lasers to construct an optically-pumped NH_3 laser involving two input CO_2 photons and to get 16 μm laser action from the NH_3,[34] as indicated by the energy level diagram in Fig. 15. Since the two photon total tunability is about 100 MHz, the energy levels must be known to this accuracy. The 5.3 μm operation of the spin flip laser overlaps a large portion of the frequency region equal to two CO_2 laser photons.

Fig. 16 indicates the spectrum of NH_3 obtained with our spectrometer. The increased resolution of the spin flip laser produces about ten times more lines than were obtained by previous means[35] in the region where the spectra overlap. The spectrum shown consists of some ν_2 transitions, however, the majority of the lines result from the ν_4 mode[36] and the spectrum will require considerable effort to unravel.

In order to explain this spectrum and obtain some useful parameters, one would like to make accurate frequency measurements on some of the line positions. There are several accuracy levels and techniques that can be used here.

One method which has been used at Heriot Watt[37] and could be put to use here is to use a known calibrant (the NO spectrum in Fig. 11 for example) along with a low finesse Fabry Perot cavity for interpolation. The unknown spectrum is compared with the calibrant over identical pump frequency and magnetic field regions.

A preferable but more difficult technique (and the one we are working toward here) is to replace the wavelength metrology with frequency metrology by a incorporating the frequency synthesis technology into the system.
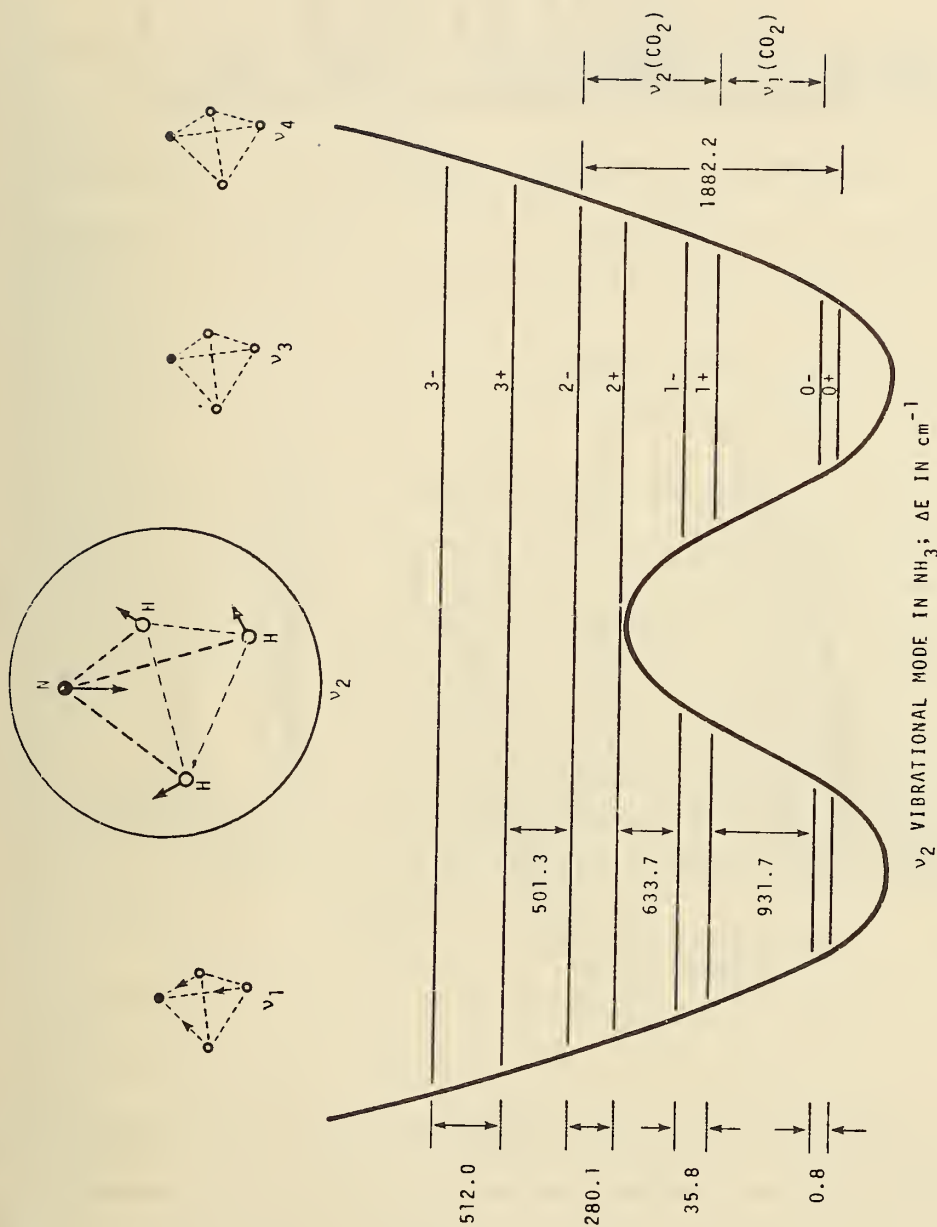
ν_2 VIBRATIONAL MODE IN NH_3; ΔE IN cm^{-1}

ν_1 ν_2 ν_3 ν_4

3-
3+
2-
2+
1-
1+
0-
0+

501.3
633.7
931.7

512.0
280.1
35.8
0.8

1882.2
$\nu_2(CO_2)$
$\nu_1(CO_2)$

Figure 15. Energy level diagram of ν_2 mode in ammonia. The ν_2 mode (encircled) generates moments along the symmetry axis, as does the ν_1 mode. The ν_3 and ν_4 modes generate moments (not indicated here) orthogonal to the symmetry axis. One particular transition of interest is from the 2+ to the 1- levels. This is a possible 16 μm laser transition which could be of considerable importance in isotope separation.
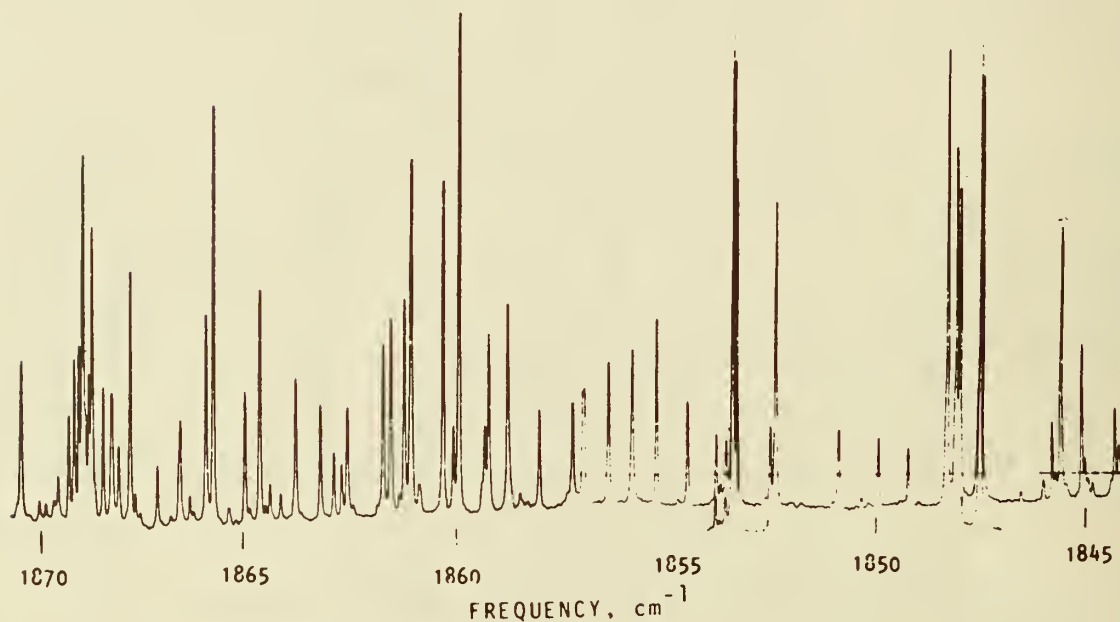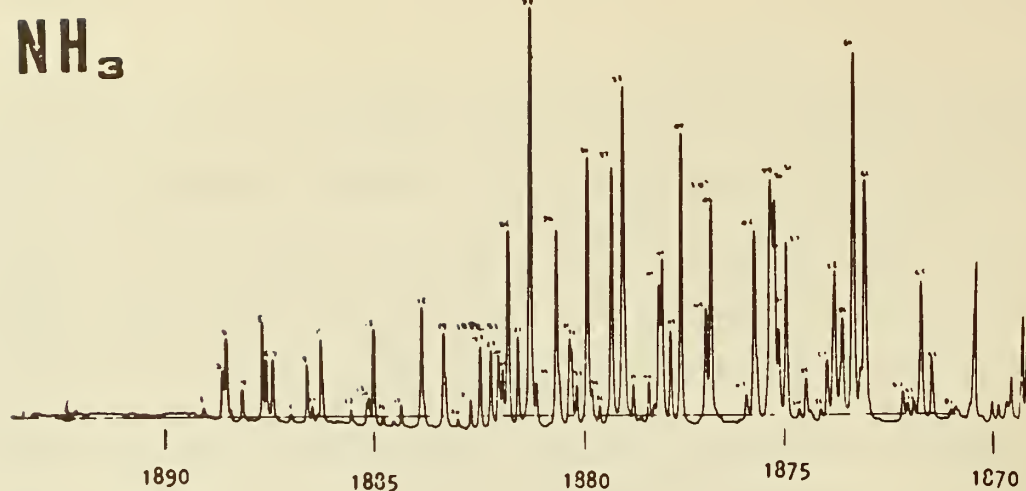
43

NH₃

Figure 16. Preliminary spectrum of 1% NH_3 in 13,300 Pa (100 Torr) N_2 mixture in opto
acoustic detector. Spectrum consists mainly of ν_4 and $2\nu_2$ transi-
tions in NH_3. The spin flip laser was operated in the quasi continuous
(spin saturated) regime with a linewidth the order of 300 MHz; a very
useful mode for survey work. Several different pump lines were used
to obtain spectra in the various 23 cm^{-1} regions that a 1 Tesla
sweep produces, then the traces were subsequently joined together. A
future improvement will consist of normalizing the absorption signals
by a ratio detection scheme in order to simplify the assignment of
transitions.

A block diagram for a scheme currently under investigation is shown in Fig. 17. The spin flip laser is tuned to some resonance feature in the gas under investigation, and the spin flip laser frequency is measured relative to the CO pump frequency. The CO pump frequency is known since it is frequency locked to a CO_2 based reference. This CO laser stabilization has already been accomplished. The more difficult measurement is the CO - SF frequency difference. Since the pump electric field and the SFRL field are presumable polarized orthogonally, the use of the Brewster angle beam splitter should effectively separate the two signals and permit one to bring the two signals to the diode independently. The major difficulty to date has been the relatively low SFRL output power. We have achieved 30 mw near resonance, but the power drops off toward longer wavelengths. The diodes seem to operate reliably with about 100 mw of power focused through an F5 lens. We have succeeded in observing a rectified signal from the SFRL radiation. The amplitude of this signal was less than 100 uv.

The low power from the SFRL may be partly caused by bounce modes which approach the InSb surface internally at an angle greater critical angle and are permanently internally reflected until they come to a corner.[38] The most promising answer to the problem appears to be that of external cavity operation.[39] With this operation one expects not only higher output power, but also a narrower linewidth since bounce modes would be eliminated. An alternate solution for the CO pump-SFRL frequency difference measurement might be a fast solid state detector which requires considerably less power for operation. To date, even the best of these, however, has only 65 GHz or so bandwidth. Thus, the much wider bandwidth of the MOM diode makes it preferable at present, and we are continuing in this direction.
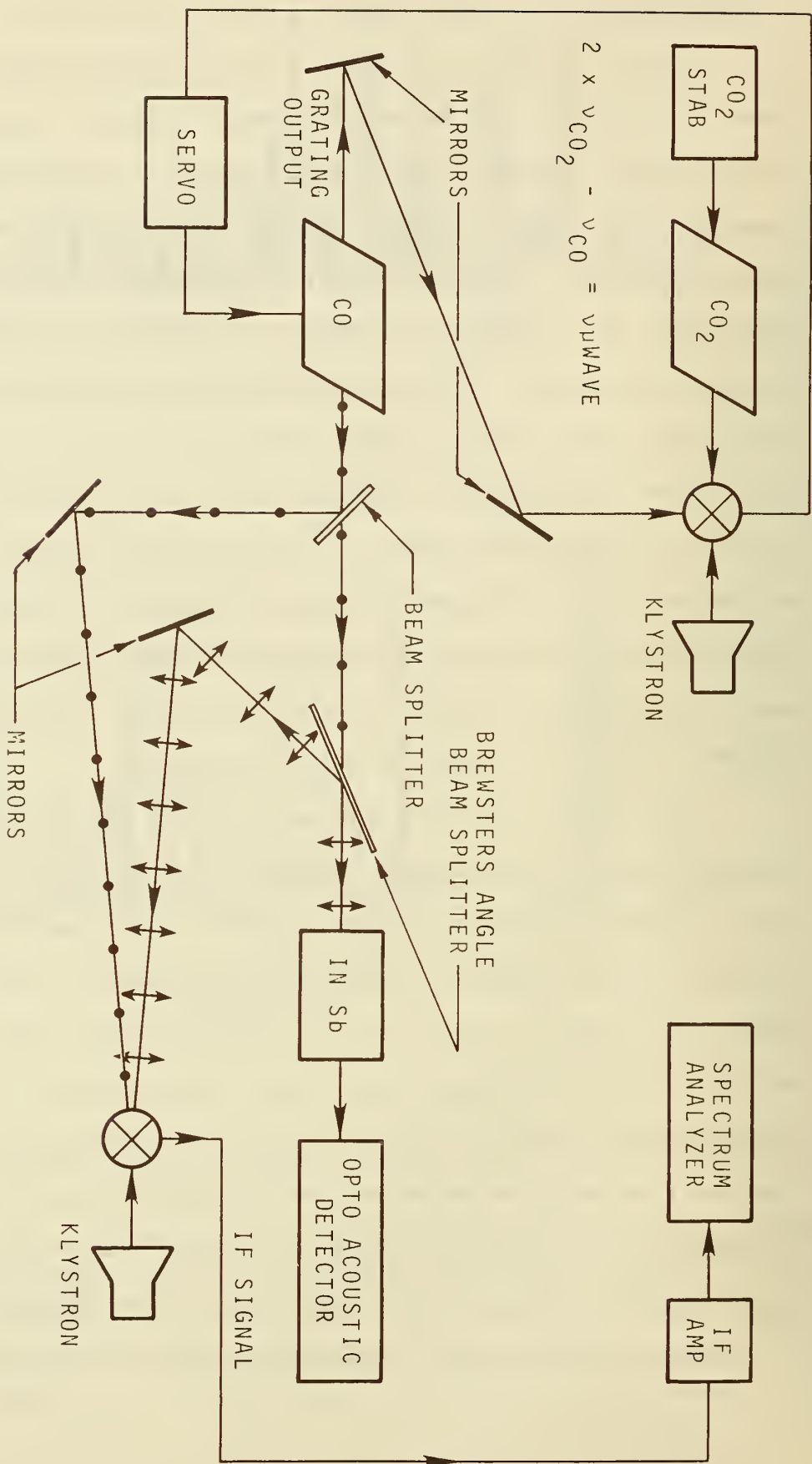
Figure 17. Block diagram of absolute frequency measurement technique under development. The CO frequency determination occurs in the laser stabilization process. In the proposed scheme above, the Brewster's angle beam splitter should allow the pump power to be transmitted unreflected, while reflecting about 80% of the spin flip power (polarized orthogonal to the pump power) to the diode. The pump power is directed to the diode by an independent path to allow optimum coupling for each signal.

46

In summary, we make the following points about the spectrometer:

1. The system has developed to the point where the spin flip laser operation is routine, and further improvements in performance require external cavity operation. 2. The present system is useful for survey work where operation is in the spin saturation mode and tuning is quasi continuous with a linewidth of about 300 MHz. 3. The system can now be operated in a mode modulated fashion with a resolution of better than 0.01 cm^{-1}. 4. By using a ratio detection scheme now on hand, one can measure chemical reaction rates if one of the reactants has a spectral feature in the 1900-1840 cm^{-1} region. 5. An additional effort is required to develop the absolute frequency measurement capability.

8. REFERENCES

1. Smith, S. D., "High resolution infra-red spectroscopy: the spin-flip laser" invited paper at the Rank Fund Symposium on Very High Resolution Spectroscopy at the Royal Society, London 5-6 Sept. 1974, Heriot Watt Physics Dept., Heriot Watt University, Riccarton, Currie, Edinburgh, Scotland.

2. Guerra, M. A., Brueck, S. R. J., and Mooradian, A., "Gradient-field permanent-magnet spin-flip laser," IEEE J. Quantum Electronics, Vol. QE-9, No. 12, Dec. 1973, pp 1157-1158.

3. Evenson, K. M., Wells, J. S., Petersen, F. R., Danielson, B. L., and Day, G. W., "Accurate frequencies of molecular transitions used in laser stabilization: the 3.39 μm transitions in CH_4 and the 9.33 and 10.18 μm transitions in CO_2," Appl. Phys. Lett., Vol. 22, No. 3, Feb. 1973, pp. 192-195.

4. Petersen, F. R., McDonald, D. G., Cupp, J. D., and Danielson, B. L. "Rotational constants for $^{12}C^{16}O_2$ from beats between Lamb-dip stabilized lasers," Phys. Rev. Lett. Vol. 31, pp. 573-576, 1973.

5. Freed, C., and Javan, A., "Standing-wave saturation resonances in the CO_2 10.6 μm transitions observed in a low-pressure room-temperature absorber gas," Appl. Phys. Lett., Vol. 17, 1970, pp. 53-56.

6. Goldan, P. D., and Goto, K., "An acoustically resonant system for detection of low level infra-red absorption in atmospheric pollutants," J. Appl. Physics, Vol. 45, No. 10, Oct. 1974, pp. 4350-4355.

7. Brueck, S. R. J., and Mooradian, A., "Near resonance spin-flip scattering in indium antimonide," Phys. Rev. Lett. Vol. 28, No. 3, Jan. 1972, pp. 161-165.

8. Patel, C. K. N., "Tunable spin-flip Raman laser at magnetic field as low as 400 G," Appl. Phys. Lett., Vol. 19, No. 10, Nov. 1971, pp. 400-403.

9. Allwood, R. L., Dennis, R. B., Firth, W. J., Smith, S. D., Wherret, B. S. and Wood, R. A., "A tunable spin-flip magneto-Raman infra-red laser," The Radio and Electronic Engineer, Vol. 42, No. 5, May 1972, pp. 243-246.

10. Brueck, S. R. J., and Mooradian, A., "Frequency stabilization and fine-tuning characteristics of a cw InSb spin-flip laser," IEEE J. Quantum Electronics, Vol. QE-10, No. 9, Sept. 1974, pp. 634-641.

11. MacKenzie, H. A., Smith, S. D., and Dennis, R. B., "Tunning and mode characteristics at the cw InSb spin-flip Raman laser determined by use of a Fabry-Perot interferometer," to be published.

12. Dennis, R. B., Pidgeon, C. R., Smith, S. D., Wherret, B. S., and Wood, R. A., "Stimulated spin-flip scattering, a magnetically tunable infra-red laser I," Proc. Psy. Soc. London, Vol. 331, No. 1585, Dec. 1972, pp. 203-236.

13. Brueck, S. R. J., and Mooradian, A., "Efficient, single-mode, cw, tunable spin-flip Raman laser," Appl. Phys. Lett. Vol. 18, No. 6, March 1971, pp. 229-230.

14. Wherrett, B. S., and Firth, W. J., "Spin saturation and pump depletion in continuous spin-flip Raman oscillation," IEEE J. Quantum Electron. Vol. QE-8, Dec. 1972, pp. 865-868.

15. Scott, J. F., "Spin-flip light scattering and spin-flip lasers," Lectures in 1973 Summer School in Crystal Mountain, Washington, Book, Physics of Quantum Electronics, Vol. II; Laser Applications to Optics and Spectroscopy, pp. 123-180, Ed. S. F. Jacobs, M. Sargent, III, J. F. Scott and M. O. Scully (Addison-Wesley Pub. Co., Inc., Reading, Mass. 1975).

16. Colles, M. J., Dennis, Smith, J. W., and Webb, J. S., "A study of factors affecting the InSb cw spin-flip laser," Optics Communications Vol. 10, No. 2, Feb. 1974, pp. 145-148.

17. Phelan, R. J., private communication.

18. Mantz, A. W., Maillard, J.-P., Roh, W. B., and Rao, K. N., "Ground state molecular constants of $^{12}C^{16}O$," J. Mol. Spectrosc. $\underline{57}$, 155 (1975).

19. Loewin, E. G., Maystre, D., McPhedran, R. C., and Wilson, I., "Correction between efficiency of diffraction gratings and theoretical calculations over a wide range," Proc. ICO Conf. Opt. Methods in Sci. and Ind. Meas., Tokyo, 1974, Japan J. Appl. Phys. 14, 1975, pp. 143-152.

20. Freed, C., "Sealed-off operation of stable CO lasers," Appl. Phys. Lett. Vol. 18, No. 10, May 1971, pp. 458-461.

21. Petersen, F. R., et al., "Far infra-red frequency synthesis with stabilized CO_2 lasers: accurate measurements of the water vapor and methyl alcohol laser frequencies," IEEE J. Quant. Electron. Vol. QE-11, No. 10, Oct. 1975, pp. 838-843.

22. Jennings, D. A., Petersen, F. R., and Evenson, K. M., "Extension of absolute frequency measurements to 148 THz: frequencies of the 2.0 and 3.5 μm Xe laser," Appl. Phys. Lett. Vol. 26, No. 9, May 1975, pp. 510-511.

23. Sakuma, E., and Evenson, K. M., "Characteristics of tungsten-nickel point contact diodes used as laser harmonic-generator mixers," IEEE J. Quant. Electron. Vol. QE-10, No. 8, Aug. 1974, pp. 599-603.

24. Hocker, L. O., Javan, A., Rao, D. Ramachandra, Frenkel, L., and Sullivan, T., "Absolute frequency measurement and spectroscopy of gas laser transitions in the far infra-red," Appl. Phys. Lett., vol. 10, No. 5, March 1967, pp. 147-149.

25. Wells, J. S., Evenson, K. M., Day, G. W., and Halford, Donald, "Role of infra-red frequency synthesis in metrology," Proc. IEEE, Vol. 60, No. 5, May 1972, pp. 621-623.

26. Matarrese, L. M., and Evenson, K. M., "Improved coupling to infrared whisker diodes by use of antenna theory," Appl. Phys. Lett., Vol. 17, No. 1, July 1970, pp. 8-10.

27. Faris, S. M., and Gustafson, T. K., "Harmonic mixing characteristics of metal-barrier-metal junctions as predicted by electron tunnelling," Appl. Phys. Lett. Vol. 25, No. 10, Nov. 1974, pp. 544-547.

28. Simmons, J. G., "Electric tunnel effect between dissimilar electrodes separated by a thin insulating film," J. Appl. Phys. 34, June 1963, pp. 2581-1590.

29. James, T. C., and Thiebault, R. J., "Spin-orbit coupling constant of nitric oxide. Determination from fundamental and satellite band origins," J. Chem. Phys. Vol. 41, 1964, pp. 2806-2813.

30. Howard, C. J., and Evenson, K. M., "Laser magnetic resonance study of the gas phase reactions of OH with CO, NO, and NO_2," J. Chem. Phys. Vol. 61, No. 5, Sept. 1974, pp. 1943-1952.

31. Nill, K. W., Blum, F. A., Calawa, A. R., and Harman, T. C., "Observation of Λ-Doubling and Zeeman splitting in the fundamental infrared absorption band of nitric oxide," Chem. Phys. Lett. Vol. 14, No. 2, May 1972, pp. 234-238.

32. Flicker, H., private communication.

33. Bischel, W. K., Kelly, P. J., and Rhodes, C. K., "Observation of doppler-free two-photon absorption in the ν_3 bands of CH_3F," Phys. Rev. Lett. Vol. 34, No. 6, Feb. 1975, pp. 300-303.

34. Rhodes, C. K., private communication.

35. Garing, J. S., Nielsen, H. H., and Rao, K. N., "The low-frequency vibration rotation bands of the ammonia molecule," J. Mole. Spectrosc. Vol. 3, 1959, pp. 496-527.

36. Maki, A. G., private communication.

37. Butcher, R. J., Dennis, R. B., and Smith, S. D., "The tunable spin-flip Raman laser, II continuous wave molecular spectroscopy," to be published in the Proc. Royal Society (London 1975).

38. Mooradian, A., lecture notes at Scottish University Summer School in Physics, Edinburg, Scotland, Aug. 1975.

39. Scragg, T., and Smith, S. D., "External cavity operation of the spin-flip Raman laser," to be published in proceedings of the Megeve Conference on High Resolution Spectroscopy, June 1975.

NBS-114A (REV. 7-73)

U.S. DEPT. OF COMM. BIBLIOGRAPHIC DATA SHEET	1. PUBLICATION OR REPORT NO. NBS TN 670	2. Gov't Accession No.	3. Recipient's Accession No.

4. TITLE AND SUBTITLE An Infrared Spectrometer Utilizing a Spin Flip Raman Laser, IR Frequency Synthesis Techniques, and CO_2 Laser Frequency Standards	5. Publication Date January 1976
	6. Performing Organization Code 277.03

7. AUTHOR(S) J. S. Wells, F. R. Petersen, G. E. Streit, P. D. Goldan and C. M. Sadowski	8. Performing Organ. Report No.

9. PERFORMING ORGANIZATION NAME AND ADDRESS NATIONAL BUREAU OF STANDARDS DEPARTMENT OF COMMERCE WASHINGTON, D.C. 20234	10. Project/Task/Work Unit No. 2773153
	11. Contract/Grant No.

12. Sponsoring Organization Name and Complete Address (Street, City, State, ZIP) National Bureau of Standards Department of Commerce Washington, D.C. 20234	13. Type of Report & Period Covered
	14. Sponsoring Agency Code

15. SUPPLEMENTARY NOTES

16. ABSTRACT (A 200-word or less factual summary of most significant information. If document includes a significant bibliography or literature survey, mention it here.)

The central part of this spectrometer is a cw spin flip Raman laser which operates between 1900 and 1800 cm^{-1}. The spin flip laser has so far demonstrated capabilities of resolving spectra separated by 0.01 cm^{-1} and shows promise of exceeding this resolution capability. When used with an opto-acoustic detector or with a detector and a flow system, it is capable of making a variety of measurements of environmental interest. Many of these environmental applications require only wavelength metrology.

By using CO_2 laser standards as frequency references and incorporating infrared frequency synthesis techniques, spectroscopy with the spin flip Raman laser can be put on a frequency metrology basis. A CO_2 laser has been used with a metal-oxide-metal diode to synthesize a known frequency reference which was used to stabilize the CO pump laser. The MOM diode also has the potential for measuring the frequency difference between the SFRL and the CO pump laser, a step which will complete absolute frequency measurements with the SFRL. The progress toward achieving this goal, the potential capabilities of this unique spectrometer, and some future applications are discussed.

17. KEY WORDS (six to twelve entries; alphabetical order; capitalize only the first letter of the first key word unless a proper name; separated by semicolons)

Air quality measurements; improved resolution spectroscopy; infrared frequency measurements; infrared spectrometer; spin flip laser; tunable IR laser.

18. AVAILABILITY	[X] Unlimited	19. SECURITY CLASS (THIS REPORT) UNCLASSIFIED	21. NO. OF PAGES 54
[ ] For Official Distribution. Do Not Release to NTIS			
[X] Order From Sup. of Doc., U.S. Government Printing Office Washington, D.C. 20402, SD Cat. No. C13, 46:670		20. SECURITY CLASS (THIS PAGE) UNCLASSIFIED	22. Price $1.60
[ ] Order From National Technical Information Service (NTIS) Springfield, Virginia 22151			

USCOMM-DC 29042-P74

☆ U.S. GOVERNMENT PRINTING OFFICE: 1975 — 677-317 / 1240 REGION NO. 8

NBS TECHNICAL PUBLICATIONS

PERIODICALS

JOURNAL OF RESEARCH reports National Bureau of Standards research and development in physics, mathematics, and chemistry. It is published in two sections, available separately:

• **Physics and Chemistry (Section A)**

Papers of interest primarily to scientists working in these fields. This section covers a broad range of physical and chemical research, with major emphasis on standards of physical measurement, fundamental constants, and properties of matter. Issued six times a year. Annual subscription: Domestic, $17.00; Foreign, $21.25.

• **Mathematical Sciences (Section B)**

Studies and compilations designed mainly for the mathematician and theoretical physicist. Topics in mathematical statistics, theory of experiment design, numerical analysis, theoretical physics and chemistry, logical design and programming of computers and computer systems. Short numerical tables. Issued quarterly. Annual subscription: Domestic, $9.00; Foreign, $11.25.

DIMENSIONS/NBS (formerly Technical News Bulletin)—This monthly magazine is published to inform scientists, engineers, businessmen, industry, teachers, students, and consumers of the latest advances in science and technology, with primary emphasis on the work at NBS. The magazine highlights and reviews such issues as energy research, fire protection, building technology, metric conversion, pollution abatement, health and safety, and consumer product performance. In addition, it reports the results of Bureau programs in measurement standards and techniques, properties of matter and materials, engineering standards and services, instrumentation, and automatic data processing.

Annual subscription: Domestic, $9.45; Foreign, $11.85.

NONPERIODICALS

Monographs—Major contributions to the technical literature on various subjects related to the Bureau's scientific and technical activities.

Handbooks—Recommended codes of engineering and industrial practice (including safety codes) developed in cooperation with interested industries, professional organizations, and regulatory bodies.

Special Publications—Include proceedings of conferences sponsored by NBS, NBS annual reports, and other special publications appropriate to this grouping such as wall charts, pocket cards, and bibliographies.

Applied Mathematics Series—Mathematical tables, manuals, and studies of special interest to physicists, engineers, chemists, biologists, mathematicians, computer programmers, and others engaged in scientific and technical work.

National Standard Reference Data Series—Provides quantitative data on the physical and chemical properties of materials, compiled from the world's literature and critically evaluated. Developed under a world-wide program coordinated by NBS. Program under authority of National Standard Data Act (Public Law 90-396).

NOTE: At present the principal publication outlet for these data is the Journal of Physical and Chemical Reference Data (JPCRD) published quarterly for NBS by the American Chemical Society (ACS) and the American Institute of Physics (AIP). Subscriptions, reprints, and supplements available from ACS, 1155 Sixteenth St. N. W., Wash. D. C. 20056.

Building Science Series—Disseminates technical information developed at the Bureau on building materials, components, systems, and whole structures. The series presents research results, test methods, and performance criteria related to the structural and environmental functions and the durability and safety characteristics of building elements and systems.

Technical Notes—Studies or reports which are complete in themselves but restrictive in their treatment of a subject. Analogous to monographs but not so comprehensive in scope or definitive in treatment of the subject area. Often serve as a vehicle for final reports of work performed at NBS under the sponsorship of other government agencies.

Voluntary Product Standards—Developed under procedures published by the Department of Commerce in Part 10, Title 15, of the Code of Federal Regulations. The purpose of the standards is to establish nationally recognized requirements for products, and to provide all concerned interests with a basis for common understanding of the characteristics of the products. NBS administers this program as a supplement to the activities of the private sector standardizing organizations.

Federal Information Processing Standards Publications (FIPS PUBS)—Publications in this series collectively constitute the Federal Information Processing Standards Register. Register serves as the official source of information in the Federal Government regarding standards issued by NBS pursuant to the Federal Property and Administrative Services Act of 1949 as amended, Public Law 89-306 (79 Stat. 1127), and as implemented by Executive Order 11717 (38 FR 12315, dated May 11, 1973) and Part 6 of Title 15 CFR (Code of Federal Regulations).

Consumer Information Series—Practical information, based on NBS research and experience, covering areas of interest to the consumer. Easily understandable language and illustrations provide useful background knowledge for shopping in today's technological marketplace.

NBS Interagency Reports (NBSIR)—A special series of interim or final reports on work performed by NBS for outside sponsors (both government and non-government). In general, initial distribution is handled by the sponsor; public distribution is by the National Technical Information Service (Springfield, Va. 22161) in paper copy or microfiche form.

Order NBS publications (except NBSIR's and Bibliographic Subscription Services) from: Superintendent of Documents, Government Printing Office, Washington, D.C. 20402.

BIBLIOGRAPHIC SUBSCRIPTION SERVICES

The following current-awareness and literature-survey bibliographies are issued periodically by the Bureau:
Cryogenic Data Center Current Awareness Service

A literature survey issued biweekly. Annual subscription: Domestic, $20.00; foreign, $25.00.

Liquefied Natural Gas. A literature survey issued quarterly. Annual subscription: $20.00.

Superconducting Devices and Materials. A literature survey issued quarterly. Annual subscription: $20.00. Send subscription orders and remittances for the preceding bibliographic services to National Bureau of Standards, Cryogenic Data Center (275.02) Boulder, Colorado 80302.

Electromagnetic Metrology Current Awareness Service Issued monthly. Annual subscription: $24.00. Send subscription order and remittance to Electromagnetics Division, National Bureau of Standards, Boulder, Colo. 80302.

1298